Screening the MMV Pathogen Box against *Toxoplasma gondii* Tachyzoites and Bradyzoites Identifies Dually Cidal *bc1*-complex Inhibitors

Deborah Maus[1], Elyzana Putrianti[1], Frank Seeber[2], Martin Blume[1*]

[1]P6: Metabolism of Microbial Pathogens, Robert Koch Institute, 13353, Berlin, Germany

[2]FG16: Mycotic and Parasitic Agents and Mycobacteria, Robert Koch Institute, 13353, Berlin, Germany

*corresponding author

Martin Blume
Project Group 6
Robert Koch Institute
Seestr. 10
13353 Berlin
Germany
Email: blumem@rki.de

Abstract

The apicomplexan parasite *Toxoplasma gondii* infects 25-30% of the global human population and can cause life-threatening diseases in immunocompromised patients. The chronic infectious form of the parasite, bradyzoites, persist within cysts in brain and muscle tissues and are responsible for its transmission and remission. Currently available treatment options are very limited and include antimicrobials currently in development novel developmental treatments. They are only effective against the fast replicating tachyzoites but fail to eradicate the chronic stages of *T. gondii*. The cause of these treatment failures remains unclear. We utilized the recently developed human myotube-based culture model to screen compounds from the MMV Pathogen Box against pan-drug tolerant *in vitro* bradyzoites. We identified various hit compounds that show simultaneous activity against tachyzoites and bradyzoites. Stable isotope-resolved metabolic profiling identified the mitochondrial bc1-complex as a target of bradyzocidal compounds. Comparing the impact of bradyzocidal with non-bradyzocidal coenzyme Q analogs on parasite ATP levels suggests active and essential mitochondrial ATP production in mature bradyzoites.

Key Words

Toxoplasma gondii, in vitro tissue cysts, MMV Pathogen Box, metabolomics, mitochondrial metabolism

Introduction

Toxoplasma gondii is an ubiquitous apicomplexan parasite that infects virtually all warm-blooded animals including 25-30 % of humans (Montazeri et al. 2020). Toxoplasmosis was ranked third in Europe in the WHO's estimates of the worldwide burden of 31 foodborne diseases, accounting for up to 20% of the overall burden (Havelaar et al. 2015). Although most acute infections caused by the tachyzoite stage of the parasite remain asymptomatic in immunocompetent individuals, the parasite persists life-long in the form of encysted semi-dormant bradyzoites (Weiss and Dubey 2009). Currently, no medical treatment exists to eradicate these cysts from infected individuals. *T. gondii* is transmitted through undercooked meat products of infected livestock but also through feline-shed oocysts that contaminate water sources and soil (Weiss and Dubey 2009). Severe toxoplasmosis occurs after reactivation of cysts or primary infection of immunosuppressed individuals or fetuses of seronegative mothers and can lead to systemic infections, uveitis, encephalitis as well as congenital transmission. If untreated, it is potentially fatal (Montoya and Liesenfeld 2004). Hence, tissue cysts of *T. gondii* constitute a long-term source for transmission and risk of acute disease. Related cyst-forming coccidians such as *Neospora caninum* and *Besnoitia besnoiti* pose an immense veterinary burden for similar reasons and cause abortion in cattle and severe chronic infection in cattle and horses, respectively. Current treatment options exist only against the tachyzoite form of the parasite and include antifolates, such as pyrimethamine or trimethoprim, that inhibit the bifunctional dihydrofolate reductase-thymidylate synthetase, in combination with sulfadiazine, which blocks the dihydropteroate synthetase. These enzymes are implicated in DNA synthesis in both the parasite and side-effects often require pre-mature abortion of the treatment (Katlama, De Wit, et al. 1996; Alday and Doggett 2017). Another potent drug target in coccidians and other apicomplexan parasites such as *Plasmodium* spp. is the cytochrome *bc1*-complex in the mitochondrial respiratory chain, which is inhibited by a number of approved drugs, such as the naphthoquinones atovaquone (Meneceur et al. 2008; Nixon et al. 2013) and buparvaquone (Sharifiyazdi et al. 2012). However, both coenzyme Q analogs fail to eradicate encysted bradyzoites of *T. gondii* and *N. caninum* from the brains of infected mice after multiple weeks of treatment (Doggett et al. 2012; Müller et al. 2015; Doggett et al. 2020). Experimental inhibitors against the bc1-complex includes 1-hydroxy-2-dodecyl-4(1H)quinolone (HDQ) that inhibits the growth of asexual blood stages of the related malaria parasite *Plasmodium falciparum* (Vallières et al. 2012). However, in *T. gondii* HDQ appears to inhibit multiple mitochondrial election donors in *T. gondii* such as the alternative NAD-dehydrogenase and the dihydroorotate dehydrogenase in tachyzoites (Lin, Gross, and Bohne 2009). It does not affect mature bradyzoites in vitro (Christiansen et al. 2022), and HDQ derivatives do not clear *T. gondii* cysts from the brains of infected mice (Bajohr et al. 2010). Also, endochin-like quinolones constitute a promising series of potent bc1-complex inhibitors that are active against *T. gondii* (McConnell et al. 2018) and *Plasmodium* parasites (Song et al. 2018). However, these compounds also do not fully eradicate the cysts *in vivo* (Doggett et al. 2012). Similarly, bumped kinase inhibitors that selectively inhibit parasite calcium-dependent protein kinases in various apicomplexans fail to clear tissue cysts *in vitro* (Christiansen et al. 2022) and *in vivo* (Hulverson et al. 2019). It remains unclear whether these drug targets of tachyzoites are less fitness-conferring in bradyzoites or whether treatment failure is due to insufficient access of the drugs to tissue cysts. To date, the genetic tools available to characterize the function of essential genes in bradyzoites are limited to promoter replacements (Smith et al. 2021). No methods exist to genetically interrogate the fitness contribution of mitochondrially encoded genes such as the cytochrome b subunit of the

cytochrome bc1-complex (J.-L. Wang et al. 2016). Consequently, reverse pharmacological approaches to develop eradicating Toxoplasmosis treatments remain difficult.

To address these shortcomings, we recently developed a human myotube-based system to generate mature *T. gondii* bradyzoites displaying *in vivo* characteristics, such as resistance to multiple experimental and medical antiparasitics (Christiansen et al. 2022). Here, we report the screening of the MMV Pathogen Box against *T. gondii* tachyzoites and pan-drug tolerant bradyzoites. We identified dually active compounds with established and unsuspected modes of action. Comprehensive stable-isotope resolved LCMS analysis of metabolic fingerprints of selected compounds allowed us to confirm the *bc1*-complex as a target for bradyzocidal compounds that is vital for ATP production.

Material and Methods

Tachyzoite Culture

Pru-Δhxgprt tdTomato (John et al. 2009) (PruTom) and RH-Rep1/2-S9(33-159)-GFP (DeRocher et al. 2000; Thomsen-Zieger, Schachtner, and Seeber 2003) (RH-S9) parasites were maintained in HFF cells (BJ-5ta human foreskin fibroblasts ATCC, CRL-4001) with Dulbecco's modified Eagle's medium (DMEM) containing 25 mM glucose, 4 mM L-glutamine, 1 mM sodium pyruvate, 100 U/mL penicillin, 100 µg/mL streptomycin and 1 % heat-inactivated fetal bovine serum (FBS, Gibco) at 37°C with 10 % CO_2 (Christiansen et al. 2022).

In vitro T. gondii tissue cyst culture

The *T. gondii in vitro* cyst culture was performed as in (Christiansen et al. 2022). In short, KD3 myoblasts (Shiomi et al. 2011) were grown to 70 % confluency, followed by the induction of myotube differentiation by changing the medium to DMEM as described above but with 2% horse serum instead of FBS and additionally supplemented with 10 µg/mL human insulin, 5 µg/mL human holo-transferrin and 1.7 ng/mL Na_2SeO_3. After five days, the myotubes were infected with PruTom (MOI 0.1) in bicarbonate-free Roswell Park Memorial Institute medium (RPMI) containing 5.5 mM glucose, 50 mM HEPES, 4 mM L-glutamine, 100 U/mL penicillin, 100 µg/mL streptomycin, 2 % horse serum, 10 µg/mL human Insulin, 5 µg/mL human holo-transferrin and 1.7 ng/mL Na_2SeO_3. Cultures were incubated at 37 °C at ambient CO_2 for four weeks and the medium was changed every two to three days. A comprehensive scheme of the procedure is shown in Fig. S1.

MMV Pathogen Box Screening Procedure

All Pathogen Box compounds were stored at -20°C (Veale 2019). DMSO-solved compounds were diluted in DMEM or RPMI media and stored at 4°C until use. Host cells were grown in transparent, flat-bottom 96-well plates and infected as described above to cultivate either tachyzoites or in vitro tissue cysts. One column per plate was left uninfected to estimate fluorescence background. Four hours after infection with tachyzoites or after four weeks of bradyzoite maturation the culture medium was replaced by medium containing either 0.1 % DMSO (negative control) or 10 µM of the respective Pathogen Box compound. During the seven day treatment period the medium was renewed every two to three days. On bradyzoite cultures the medium was changed to tachyzoite growth medium to induce the re-differentiation of viable bradyzoites to tachyzoites and the culture was monitored over 28 days. Prior to each medium exchange, the cultures were inspected for compound crystallization. The fluorescence was measured in a fluorescence plate reader (Tecan Infinite M200 PRO) (excitation Λ = 554 nm, emission Λ

= 589 nm). Fluorescence values passing a threshold of 2000 after background subtraction indicated proliferating parasites, hence an ineffective treatment. Figure 1 illustrates the screening experiments.

Resazurin viability assay

Host cell monolayers were washed with PBS and incubated with 500 nM Resazurin in Milli-Q water at 37 °C for 4 hours. The fluorescence was measured (excitation Λ = 540 nm, emission Λ = 580 nm) in a fluorescence plate reader (Tecan Infinite M200 PRO) and normalized to the average fluorescence values of the DMSO-treated controls which were set at 100 %.

The dose response of dually active compounds

Tachyzoite and bradyzoite cultures were treated with the MMV compounds which were pipetted in a serial dilution across the 96 well plate and treated for 7 days. Afterwards, the compound containing medium was removed and a possible regrowth was observed for another 7 days (tachyzoite assay) or 21 to 28 days (bradyzoite assay). The gathered relative fluorescence units were background subtracted. Depending on the development of the DMSO control, a dataset that optimally reflected the dose response was chosen to calculate the half-maximal inhibitory concentration (IC_{50}) for tachyzoites and the half-maximal lethal concentration (LC_{50}) for bradyzoites. In tachyzoite datasets that time point was between day 4 and day 7. Bradyzoite cultures exhibited generally lower MOI and the chosen LC_{50} time point varied between experiments from 7 to 28 days post treatment. For an ideal LC_{50} we chose the first time points where at least one bradyzoite culture completed tachyzoite regrowth and another bradyzoite culture showed no growth and a third culture was at an intermediate stage. Figure 2A,B and figure 2C,D illustrates that procedure. Using GraphPad Prism 9, the data was transformed logarithmically and a non-linear regression (curve fit with variable slope) was performed to determine the dose response.

In silico predictions

MMV provided the SMILES IDs for every compound, which we compiled with LightBBB (Shaker et al. 2020) to predict the blood-brain permeability and SwissADME (Daina, Michielin, and Zoete 2017) to predict the gastrointestinal absorption capability. The logP values were provided by MMV.

Mitochondrial activity fluorescence stain

HFF cells were infected with RH-S9GFP parasites at MOI 0.1 and treated for 24 h with 1 µM atovaquone, 25 nM buparvaquone or 5 µM MMV1028806 corresponding to five-fold of the respective IC_{50} values or 0.1 % DMSO as a solvent control. Infected cells were then stained with 500 nM MitoTracker Deep Red FM (MT, Thermo Fisher) in DMEM for 40 min at 37 °C followed by a 20 min de-stain with DMEM and fixation with 1 % paraformaldehyde for 20 min at room temperature. Mowiol containing DAPI (1:3000) was used to mount the cells. For every condition, at least 20 fluorescence images were taken at identical exposure times (DAPI 200 ms, MT 500 ms, S9-GFP 200 ms, Brightfield 10 ms) with a Zeiss Axio Imager Z1 Microscope equipped with the ApoTome 2. Using ImageJ (Schindelin et al. 2012), the intensity

threshold of individual pixels of MT (190 to 255) and DAPI (140 to 255) channels was cut off and the signal intensity was calculated per parasitophorous vacuole.

Untargeted Metabolomics

HFF cells were infected with PruTom at MOI 1. Approximately 64 hours later, the cultures were treated with 1.5 µM MMV019189, 7 µM MMV1028806, 30 µM MMV228911, 1.2 µM MMV595321, 5 µM MMV688762, 2 µM MMV688854,respectively, and 0.1 % DMSO as a control for 3 hours. These concentrations correspond to the five-fold respective IC_{50} values. Cultures were quenched in ice-cold PBS and parasites were isolated from their host cells by passaging scraped monolayers through a 23 G needle, filtered through a 3 µm polycarbonate filter and after microscopic counting distributed at 1 x 10^8 parasites per sample. Parasites were washed with ice-cold PBS via 5 min centrifugation at 21'500 x *g* at 0 °C. Metabolites were then extracted by sonication for 2 min in 50 µL 80 % acetonitrile in water. The insoluble particles were pelleted for 5 min at 21,500 x *g* at 0 °C. 5 µL of each sample was collected to generate a pooled biological quality control (PBQC) which was injected regularly into the otherwise randomized run list. 5 µL of each sample was injected onto either an ACQUITY UPLC BEH amide column (Waters) equipped with a VanGuard amide pre-column (Waters) or onto a SeQuant ZIC-pHILIC (Merck) column with an OPTI-LYNX ZIC-pHILIC guard column cartridge (Optimize Technologies) operating on a Vanquish Flex (Thermo Fisher). Analytes were chromatographically separated starting with 100 % eluent A (90 % acetonitrile in water with 10 mM ammonium carbonate) and 0 % eluent B (10 mM ammonium carbonate in water), decreasing to 40% A and 60% B over 25 min. Metabolites were detected on a Q Exactive Plus (Thermo Fisher) equipped with an electrospray ionization source operated in rapid polarity-switching mode at an MS^1 resolution of 70k and an MS^2 resolution of 35k (Top3 MSX1). Peak extraction, retention time alignment, and peak annotation were computed with Compound Discoverer 3.1 (Thermo Fisher) using an in-house library of authentic standards, blank subtraction, gap-filling as well as statistical analysis were performed in Excel (Microsoft), and the data was plotted with GraphPad Prism 8.4.1.. Principal component analysis was performed with the free online tool ClustVis (Metsalu and Vilo 2015).

Isotopic labeling

Intracellular parasites were treated as mentioned above and incubated for three hours with DMEM containing either 25 mM U-^{13}C-glucose or 4 mM ^{15}N-amide-glutamine instead of the respective unlabeled carbon sources. Quenching, parasite isolation, metabolite extraction and liquid chromatography were performed as described. To increase coverage of the isotopologues, metabolites were measured in positive and negative mode separately without MS^2 scans but with an increased MS^1 scan resolution of 140k. For peak identification purposes, the unlabeled DMSO-treated sample was analyzed with intermittent MS^2 scans as described above.

ATP luciferase assay

PruTOM tachyzoites were cultivated in HFF cells without glucose, isolated 48 h post-infection and treated with 1 µM atovaquone or HDQ for 3 h. PruTOM bradyzoites were matured for three weeks, glucose-starved for an additional week and treated for 24 h with 1 µM atovaquone or

HDQ before being released by needle passage 23 G, pepsin digestion for 20 min at 37 °C. The digestion reaction was stopped by neutralizing in 1.2 % sodium bicarbonate (pH ≈ 8.3) with 0.0159 g/l phenol red as pH indicator dye (Christiansen et al, 2022). They were isolated by douncing on ice and filtered through a 3 µm polycarbonate filter. 10^5 parasites were then aliquoted in 100 µL ice-cold PBS in a 96-well plate. ATP was quantified using BacTiter-Glo™ Microbial Cell Viability Assay (Promega) according to the manufacturer's protocol using a standard curve. Data were plotted in GraphPad Prism 8.4.1..

Results

The Pathogen Box contains dually active compounds

To identify compounds targeting both, the tachyzoite and the bradyzoite stage of *T. gondii*, initially we tested 371 of 400 compounds from the Pathogen Box at a concentration of 10 µM against both stages. Since we wanted to focus on bradyzoite-specific compounds from this initial screen that had been previously reported to be active against *T. gondii* tachyzoites (Spalenka et al. 2018). HFF cells were infected with tachyzoites of the Pru strain expressing tandem Tomato fluorescent protein in its cytosol (PruTom) at an MOI of 1 (Fig 1A). 47 compounds completely inhibited growth during 7 days of exposure while the parasitemia of DMSO-treated controls already peaked after 4 days (Fig 1B). To also identify bradyzoidal compounds we differentiated KD3 myoblasts for one week into multinucleated myotubes and infected them under bicarbonate-deplete conditions and at a multiplicity of infection of 0.1 for four weeks to allow maturation of tissue cysts (Fig. S1). We exposed the cultures to 10 µM of the 371 MMV compounds for one week, removed the inhibitors and stimulated re-differentiation into tachyzoites by bicarbonate supplementation (Fig 1C). Growth of DMSO-treated cultures became detectable after 10 to 14 days. Interestingly, cyst treatment with 31 compounds prevented any tachyzoite regrowth (Fig 1D) indicating bradyzoidal activity. To exclude host cytotoxicity-dependent suppression of parasite growth we measured the reductive potential of myotubes and HFF cells using a resazurin cell viability assay. At 10 µM 30, 12 and 13 of the compounds inflicted cytotoxicity onto HFFs, myotubes or both cell types, respectively. Taken together, we identified 14 compounds that showed dual activity against tachyzoites and bradyzoites while exhibiting no cytotoxicity to both host cell types at the concentrations tested.

Validation of screening hits

To validate our results, we determined half-inhibitory concentrations (IC_{50}) and of dually active screening hits and in addition used previously reported tachyzoite inhibiting compounds (Spalenka et al. 2018) (Fig. 2A,B) and the half-maximal lethal concentration (LC_{50}) in bradyzoites (Fig. 2C,D). We confirmed dual activity of 16 compounds that exhibited mean IC_{50} values ranging between 70 pM and 1.1 µM for tachyzoites (Fig 2E) and higher LC_{50} values between 0.15 and 8.2 µM for bradyzoites (Fig 2F). To allow a comparison between the tachyzoite and bradyzoite data, we also determined the respective minimal lethal concentrations (MLC) over a seven day treatment duration of tachyzoites as well (Fig. 2G). Except for four compounds (MMV021013, MMV022478, MMV658988, MMV659004) minimal lethal concentrations were higher in bradyzoites, potentially reflecting their lower metabolic activity and the cyst wall as a diffusion barrier.

Dually active MMV Pathogen Box hits share high lipophilicity and are indicated to be active against other pathogens

To gain insight into other antibiotic properties of dually active compounds from our initial screen (Fig 1E), we tabulated indicated activities as provided by MMV (Fig 3A). As expected, these compounds were mostly considered active against *T. gondii* tachyzoites (67%), however, none of those compounds exhibited bradyzoidal activity. Instead, 27% of dually active compounds

were considered active against *Cryptosporidium*. Interestingly, despite the relative phylogenetic proximity of *P. falciparum* only 5% of the 125 potential antimalarials blocked growth of both *T. gondii* stages. To characterize physicochemical properties of these dually active hits, we compared their logP values as proxies for their lipophilicity to exclusively compounds that were inactive or active against a single *T. gondii* stage (Fig 3B). We found that tachyzoidal compounds possess a significantly higher lipophilicity than the average Pathogen Box compounds and this trend was more accentuated for bradyzoidal and dually active compounds. We estimated permeability through the blood brain barrier (bbb) using LightBBB (Shaker et al. 2020) and gastrointestinal absorbability (GIA) using swissADME (Daina, Michielin, and Zoete 2017). Most of the dually active drugs were predicted to be both permeable across the bbb and absorbed in the intestine. Together, these data indicate that phylogenetic relationship is not a dominant predictor of activity of Pathogen Box compounds against *T. gondii* bradyzoites and that lipophilicity may play an important role.

Metabolomic response of tachyzoites indicates conserved and novel modes of action

To characterize the modes of action of confirmed dually active hits we chose five compounds that had a yet unknown mode of action and were available in sufficient quantities to treat intracellular parasites and record their metabolic responses (Fig. 4 and Supplemental File 1). We treated heavily infected monolayers for three hours with a 3-fold of respective IC_{50} concentrations of MMV-compounds or the solvent DMSO. The inhibitor MMV688854 (BKI 1294) (Doggett et al. 2014) is considered to inhibit a non-metabolic target (calcium-dependent protein kinase (CDPK1)) at the employed concentration (Hayward et al. 2023) and served as an additional control to estimate generic metabolic responses of *T. gondii* to growth inhibition. We filter-purified parasites from quenched monolayers and analyzed their acetonitrile extracts by LCMS using both, pHILIC and BEH-amide chromatography columns. We repeated the experiment three times, generating 3 replicates per treatment, yielding in 9 samples per condition in total. A principal component analysis illustrates that batch to batch effects are the main contributors to biological variances within the dataset (Fig. 4A,B). Despite that, all compounds elicited a distinct metabolic phenotype on both LCMS systems (Fig 4C). The non-metabolic control inhibitor increased levels of AMP, oxidized glutathione, pseudouridine, citrulline, glycolate and glutamyl glutamine, while reducing the abundances of GABA, carbamoyl aspartate, phosphoenolpyruvate and a hexose phosphate. Shifts in these metabolites are shared among many treatments and indicate their implication in a general stress response and do not signify direct interference with parasite metabolism.

Inhibitor-specific responses include the accumulation of cGMP-AMP after treatment with MMV019189, accumulation of carbamoyl aspartate and dihydroorotate upon MMV1028806 treatment and a general depletion of central carbon metabolites (PEP, succinate, citrate, glyceraldehyde 3-phosphate, ATP, MEP) in MMV228911-treated parasites. MMV595321 caused a rather specific accumulation of N-acetylated amino acids and MMV688762 led to uracil deficiency and an accumulation of dihydroorotate and orotate. These data suggest that MMV inhibitors cause a bipartite metabolic response composed of generic and compound-specific changes.

MMV1028806 and buparvaquone target the bc1-complex in *T. gondii* similar to atovaquone.

The metabolic impact of most tested MMV compounds indicated a novel mode of action that did not resemble recognizable metabolic fingerprints. However, the metabolic fingerprint of MMV1028806 was consistent with inhibition of pyrimidine biosynthesis at the bc1-complex-dependent oxidation of dihydroorotate to orotate as has been reported for *P. falciparum* (Allman et al. 2016; Creek et al. 2016; Antonova-Koch et al. 2018). A similar response would be expected to MMV689480 (buparvaquone) which we found to be dually active against *T. gondii* tachyzoites and bradyzoites, targets the bc1-complex in *Theileria annulata* (McHardy et al. 1985), *Neospora caninum* (Müller et al. 2015) and was recently found active against *T. gondii* tachyzoites (Hayward et al. 2023).

To test these hypotheses we exposed intracellular parasites to MMV1028806 or buparvaquone (BPQ) while substituting the carbon source glucose by ^{13}C6-glucose for three hours. We then measured the incorporation of ^{13}C into the central carbon metabolism as well as the pyrimidine synthesis pathway. As controls we utilized the known bc1-complex inhibitor atovaquone (ATQ) and the solvent DMSO. All three treatments led to a drastic accumulation of carbamoyl aspartate and dihydroorotate which was accompanied by a depletion of uracil and uridine, in particular of the +5 labeled uridine isotopologue. These changes are consistent with impaired function of the bc1-complex-dependent dihydroorotate dehydrogenase (Fig 5A,B). Another common effect was the accumulation of succinate and depletion of fumarate that also indicates impaired removal of electrons from $FADH_2$ via the bc1-complex. Inhibitor-specific changes include the lower label incorporation into aconitate and depletion of its abundance by ATQ and BPQ. These compounds but not MMV1028806 allowed continued anaplerotic replenishing of succinate fumarate and malate levels as suggested by the presence of the M+3 isotopologue. In contrast, MMV1028806-treated parasites continue to generate citrate and aconitate via citric acid synthetase as shown by enrichment in its M+2 isotopologue but exhibit diminished analplerotic synthesis dicarboxylic acids in the reductive branch of the TCA-cycle. Anaplerotic substrates were also affected by all three treatments. Most notable is a strong accumulation of aspartic acid. Interestingly, pyruvate was depleted by ATQ and MMV1028806 but accumulated by BPQ. Together, these data show that all three treatments lead to the accumulation of metabolites upstream of the bc1-complex-dependent reaction in pyrimidine synthesis and the depletion of pyrimidines (Fig. 5C). Consequences of bc1-complex inhibition on the TCA cycle appear inhibitor-specific and may reflect disparate inhibition kinetics, distinct cytochrome c inhibition sites or additional coenzyme Q dependent targets.

To independently confirm our results we hypothesized that *T. gondii* also incorporates glutamine-derived nitrogen into pyrimidines. We replaced glutamine with its ^{15}N-amide-labeled isotopologue in the tachyzoite culture media for three hours while simultaneously exposing the parasites to ATQ, BPQ and MMV1028806. As expected from our previous experiments, we observed a marked decrease of uracil and uridine levels while aspartate, carbamoyl aspartate and dihydroorotate accumulated (Fig 6A). Consistently, ^{15}N-incorporation into pyrimidines was diminished while carbamoyl aspartate and dihydroorotate were heavily labeled as M+1 isotopologues (Fig 6B). These results indicate that the amide moiety of glutamine presents a major nitrogen source for pyrimidines and agree with our previous findings in that the impact of MMV1028806 and BPQ on the pyrimidine biosynthesis pathway mirrors the one of ATQ (Fig. S2).

Atovaquone, buparvaquone and MMV1028806 deplete the mitochondrial membrane potential of tachyzoites.

The inhibition of the bc1-complex by ATQ leads to the collapse of the mitochondrial membrane potential in *T. gondii* tachyzoites (Vercesi et al. 1998) and we anticipate a similar phenotype in BPQ and MMV1028806-treated parasites. We treated intracellular tachyzoites for 24 h with the three inhibitors or 0.1 % DMSO alone and estimated the mitochondrial membrane potential and morphology using a fluorescent mitotracker dye. The mitochondria of control parasites appeared as extended loops but largely collapsed after treatments with all three compounds (Fig 7A). To compare the membrane potentials of parasite mitochondria between the treatments, we calculated the ratio of total mitotracker fluorescence per vacuole and the total DAPI fluorescence serving as a proxy for total parasite DNA (Fig 7B). Expectedly, ATQ, BPQ and MMV1028806 reduced this ratio to similar extents as compared to controls.

The differential efficacy of atovaquone and HDQ against bradyzoites correlates with the inhibition of ATP levels in bradyzoites

ATQ and 1-hydroxy-2-dodecyl-4(1)quinolone (HDQ) are both coenzyme Q analogs with distinct drug targets. While ATQ inhibits the bc1-complex, HDQ inhibits dihydroorotate dehydrogenase (DHOD) (Hegewald, Gross, and Bohne 2013) and the alternative NADH dehydrogenase (NDH2) (Saleh et al. 2007). Both compounds block tachyzoite growth at low nanomolar concentrations *in vitro* (Fig 8A). However, in contrast to ATQ, HDQ does not affect the viability of mature *T. gondii* bradyzoites despite diminishing their mitochondrial membrane potential (Christiansen et al. 2022). Bradyzoites treated with up to 20 µM HDQ did readily re-differentiate into tachyzoite after treatment, while bradyzoites that were treated with at least 5 µM ATQ did not convert to proliferating tachyzoites (Fig 8B). To investigate how these modes of actions inhibit the mitochondrial transport chain in bradyzoites, we tested their influence on mitochondrial ATP production by luciferase-based ATP assay. This assay shows a linear response to parasite cell equivalents between 10^3 and 10^6 parasites per 100 µL, and in order to minimize variance we decided to work with 10^5 parasites. We starved three week old bradyzoites for one week of glucose. As a comparison we utilized tachyzoites that were cultured for two days in glucose-deplete conditions. Untreated tachyzoite samples contained in average 196 fmol ± 21 fmol ATP per 10^5 parasites, whereas untreated bradyzoites only contained 14.1 fmol ± 1.1 fmol. (Fig. 8C). Three hour ATQ treatment decreased ATP levels in both stages by 75 % (Fig 8D). In tachyzoites, HDQ also reduced ATP levels by 60 % (Fig 8D), but bradyzoites were less affected and the amount of ATP dropped down only by 14 % (Fig 8D). This indicates that bradyzoites maintain very low ATP levels and is consistent with the presence of a diminished but obligate mitochondrial ATP production that functions independently of exogenous glucose and HDQ-target enzymes.

Discussion

Summary

New treatment options for chronic *T. gondii* infections are needed because so far chronic infections cannot be cured and currently available treatments of acute toxoplasmosis are associated with severe side-effects in particular in infants after congenital transmission (Konstantinovic et al. 2019). To foster the identification of drug targets and promising compounds simultaneously, we exploited a recently developed in vitro culture system of mature pan-drug tolerant bradyzoites (Christiansen et al. 2022) to screen 400 compounds of the Pathogen Box. This system differs from previously used screens by the testing of both tachyzoites and bradyzoites. We measured tachyzoite growth in presence of candidate compounds via fluorescence of tdTomate expressing parasites daily to detect parasitostatic inhibitors. We also identified bradyzocidal activity by exposing bradyzoites that matured for four weeks, for one week to inhibitors and re-differentiated these parasites. After four weeks in vitro bradyzoites develop tolerance against antifolates and other tachyzoite growth inhibitors (Christiansen et al. 2022). We confirmed cidal activity of 14 compounds against bradyzoites, with simultaneous inhibition of tachyzoite growth. Metabolic profiling and stable isotope tracing in treated tachyzoites suggested the inhibition of the mitochondrial bc1 complex by MMV1028806 and the reference compound BPQ.

The Screen in General

For our initial screen we used a concentration of 10 µM and found that 55 compounds compromised the viability of the host cell in a resazurin assay. 15 compounds of the Pathogen Box were previously found to inhibit growth of *T. gondii* tachyzoites at concentrations below 1 µM via an end-point ELISA-based assay (Spalenka et al. 2018). While we deprioritized these compounds in our initial screen, we confirmed the activity of 14 compounds against tachyzoites in a secondary screen where 10 molecules turned out to be cidal against bradyzoites as well. However, of the 15 compounds in the Toxoplasmosis disease set, as earmarked by MMV, only 10 were found to be active against tachyzoites and none against bradyzoites. These differences may be attributed to strain-specific susceptibilities which are known for anti-folates and atovaquone (Meneceur et al. 2008) and differences in growth assays. MMV assessed activities via plaque assay that prevents media change and relies visual inspection of growth of a low number of parasites and might overestimate inhibitory effects.

Lipophilicity and why it is important (DHFR)

We also checked the predicted adsorption in the gastrointestinal tract (GIA) and blood-brain-barrier permeability. A promising drug candidate would combine these two features and be active against both stages of the parasite. We found 14 of our primary hits to fit these criteria, including eight of the confirmed dually active compounds. The lipophilicity as estimated by the octanol-water partition coefficient (logP) is a predictor of membrane permeability of compounds and often considered during drug development efforts (Lipinski et al. 2001). We found that bradyzoidal compounds exhibit higher predicted logP coefficients, suggesting that the preferred mode of entry is not via active transporters but rather via diffusion across the cyst wall. Highly polar drugs such as fosmidomycin have previously been associated with poor efficacy against *T. gondii* due to a lack of parasite plasma membrane permeability (Nair et al. 2012; Baumeister et al. 2011). MMV675968 is a dually active *T. gondii* compound and has been shown to be a potent inhibitor of the dihydrofolate reductase (DHFR) in a range of pathogens (Songsungthong et al. 2019, 2021; Kim et al. 2021; Borba-Santos, Vila, and

Rozental 2020; Nugraha et al. 2019; Rollin-Pinheiro et al. 2021; Vila and Lopez-Ribot 2017; Cantillon et al. 2022). Although its target in *T. gondii* remains to be identified, pyrimethamine, which inhibits the dihydrofolate reductase-thymidylate synthetase in *T. gondii* is inactive against both in vitro and brain-resident bradyzoites (Christiansen et al. 2022; Montazeri et al. 2018). Similarly, the DHFR inhibitor trimethoprim also penetrates the blood brain barrier (Ineichen et al. 2020) does not entirely clear brain resident cysts when applied in combination with sulfamethoxazole (Enshaeieh et al. 2021). A scenario where DHFR-TS remains essential for bradyzoite viability but pyrimethamine is excluded from the cyst appears consistent with these data. Future investigations should also include DHFR inhibitors with improved bioavailability, CNS accumulation, and a higher specificity for the TgDHFR compared to human DHFR (Hopper et al. 2019). Our data suggest that diffusion barriers such as the blood-brain barrier and the cyst wall rather than dispensability of drug targets in bradyzoites may play a significant role in the apparent pan-drug tolerance of brain-resident bradyzoites.

Untargeted Metabolomics and why we used the BKI

We used metabolomics to identify the modes of actions of five inhibitors. Generally metabolic phenotypes are composed of direct consequences of target inhibitions but also indirect effects due to a decreased growth rate and general stress. We employed the bumped-kinase inhibitor MMV688854 (BKI-1294) that targets the calcium-dependent protein kinase 1, needed for invasion (Johnson et al. 2012) and also affects formation of daughter cells (Winzer et al. 2015) as a control compound to identify metabolites implicated in a general stress response. AMP and oxidized glutathione accumulated and are the most conserved responses across the six treatments and may indicate depleted energy levels and oxidative stress (Caro et al. 2012). Also pseudouridine is elevated in many treatments. Enhanced pseudouridylation of RNA is considered to be implicated in stress responses (Cerneckis et al. 2022) and modulation of RNA stability (Davis 1995). It remains to be tested which of these conserved metabolic responses towards a panel of growth inhibitors signify cellular decay and which ones take part in a productive metabolic stress response in *T. gondii*. Nonetheless, metabolic profiling data of treated cells can be used to design combination therapies, by either interfering with productive metabolic stress responses (Zampieri et al. 2017) but also by simultaneously inhibiting otherwise non-essential pathways (Campos and Zampieri 2019). The systematic identification of target structures and modes of action from profiling data alone remains challenging due to inherent non-linear relationships within the cellular metabolic network. A systematic mapping of genetic disruptions to metabolic phenotypes, as demonstrated in *E. coli,* may alleviate these restrictions (Anglada-Girotto et al. 2022).

Specific Metabolic Responses: MMV019189, MMV228911 and MMV1028806

Apart from the general metabolic stress response to the treatment with MMV688854, three compounds caused apparent inhibitor-specific signatures. MMV019189, which is known to inhibit *P. falciparum* (Duffy et al. 2017), but also *C. parvum* (Hennessey et al. 2018) and *L. mexicana* (Berry et al. 2018), lead to the accumulation of c-GMP-AMP in the parasite. The responsible enzyme in mammalian cells is the c-GMP-AMP synthase (cGAS), which senses cytosolic DNA and triggers a type-I interferon response (Sun et al. 2013). While cGas is considered absent in *T. gondii*, host c-GMP-AMP induces STING-signaling as a response to *T. gondii* infection (P. Wang et al. 2019). Hence, MMV019189 may implicate the host in its antiparasitic activity.

Another specific metabolic signature was caused by MMV228911, that has been suggested as an inhibitor of the 1-deoxy-D-xylulose 5-phosphate reductoisomerase (DXR) in *Salmonella*

enterica (Ngcongco 2020). *T. gondii* possesses such an enzyme as part of the non-mevalonate pathway in the apicoplast and the depletion of 2-C-methylerythritol 4-phosphate is consistent with DXR inhibition. Interestingly, MMV228911 caused dysregulation of central carbon metabolism marked by a decrease of many phosphorylated metabolites. A similar metabolic cross-talk between the apicoplast-resident non-mevalonate pathway and a cytosolic sugar phosphatase has been observed in Fosmidomycin resistant *Plasmodium falciparum* parasites (Guggisberg et al. 2014). *Toxoplasma gondii* DXR is also the target of fosmidomycin (Nair et al. 2012; Baumeister et al. 2011). However, due to inefficient cellular uptake it is clinically not useful for the treatment of *T. gondii* infections.

The third potential metabolic inhibitor was MMV1028806. It is known to inhibit *P. falciparum* (Duffy et al. 2017) and also *C. elegans* (Partridge et al. 2018). The most striking alteration was the simultaneous increase of carbamoyl-aspartate and dihydroorotate, which indicates a halt in pyrimidine biosynthesis at the level of dihydroorotate dehydrogenase (Hyde 2007; Asai et al. 1983). This constellation is indicative for the inhibitors of bc_1 complex , such as atovaquone, and its metabolic response is well characterized in *P. falciparum* (Allman et al. 2016; Creek et al. 2016; Antonova-Koch et al. 2018) and in *T. gondii* (Lin, Gross, and Bohne 2009; Vercesi et al. 1998).

Stable isotope labeling confirms the bc_1 complex as target of MMV1028806, BPQ and ATQ

We compared metabolic fingerprints of MMV1028806 and BPQ with ATQ-treated parasites and confirmed a sharp increase of pyrimidine synthesis substrates, depletion of pyrimidines and dysregulation of TCA cycle intermediates. This is consistent with previous mass spectrometry-based studies (Creek et al. 2016; Allman et al. 2016; Antonova-Koch et al. 2018). We confirmed the bc1 complex as a target by measuring the synthesis of TCA cycle and pyrimidine biosynthesis intermediates via the monitoring of the incorporation of ^{13}C and ^{15}N stable isotopes from glucose and glutamine, respectively. Both, the isotopologue and metabolite abundances strongly suggest attenuation of pyrimidine production and TCA cycle fluxes by all three inhibitors (Hortua Triana et al. 2016). Differences arise in the levels of citrate and pyruvate which remain unaffected by MMV1028806 and BPQ, respectively. TCA cycle intermediates show characteristic isotopologue distributions that are indicative of a ^{13}C-label incorporation via acetyl-CoA (MacRae et al. 2012). Increased M+3 isotopologue species in dicarboxylic acids in ATQ- and BPQ-treated parasites indicate enhanced anaplerotic synthesis from glycolytic intermediates under these conditions. These distinct effects may reflect additional off-target effects and differential timing of the metabolic inhibition. Independently, the mitochondrial electron transport chain of BPQ and MMV1028806 is experimentally confirmed by the disruption of the membrane potential, as measured by Mitotracker staining (Fig 7).

Interestingly, six compounds from the MMV pathogen box have recently been shown to inhibit O_2 consumption in tachyzoites through bc1-complex inhibition (Hayward et al. 2023). We co-identified Buparvaquone as a bc1-complex inhibitor but we did not test the remaining five compounds for their targets. However, in our screen at 10 µM we found MMV024397 and MMV688853 to be dually active, while Trifloxystrobin (MMV688754) and Auranofin (MMV688978) lacked inhibitory activity in bradyzoites, and Azoxystrobin (MMV021057) was inactive. In addition, the previously described bc1-complex inhibitor ELQ400 (MMV671636) (McConnell et al. 2018) was dually active. Together, these data suggest that the bc1-complex

is needed for survival of bradyzoites, while not every tachyzocidal bc1-inhibitor also inhibits bradyzoites.

HDQ and ATQ - the mystery in the mitochondria

We previously showed that another mitochondrial electron transport chain inhibitor, HDQ, inhibits tachyzoite growth while also collapsing the mitochondrial membrane potential in bradyzoites (Christiansen et al. 2022). However, even at high multiples of its tachyzoite IC_{50}, HDQ does not kill in vitro bradyzoites (Christiansen et al. 2022). To differentiate essential from non-essential roles of the mitochondrial electron transport in bradyzoites, we measured ATP concentrations in glucose-starved bradyzoites. ATP levels collapse in the presence of ATQ but not HDQ, while both compounds deplete ATP in tachyzoites (Fig 8). This suggests that mitochondrial ATP production is needed in mature bradyzoites and that HDQ does impair active but non-essential processes in bradyzoites. HDQ inhibits the bc1 complex directly in *P. falciparum* (Vallières et al. 2012). However, in *T. gondii* it blocks pyrimidine synthesis via DHOD and mitochondrial NADH oxidation via NDH2 (Lin, Gross, and Bohne 2009), while ATQ inhibits the ubiquinone reductase center of the bc1-complex in *T. gondii* directly (McFadden et al. 2000). These results also agree with the notion that the canonical TCA cycle in bradyzoites is active but not an important source of mitochondrial reduction equivalents (Christiansen et al. 2022). The nature of the electron sources to maintain the bc1-complex-dependent functions in bradyzoites remains to be established and may include HDQ-insensitive glycerol 3-phosphate dehydrogenase, succinate dehydrogenase (complex 2) and the malate:quinone oxidoreductase (Maclean et al. 2021). In young seven day-old bradyzoites, glycolysis and mitochondria both produce ATP as shown by 2-deoxyglucose and oligomycin A dependent inhibition (Fu et al. 2021; Shukla et al. 2018).

Interestingly, despite its profound effect on ATP levels and viability of bradyzoites ATQ fails to eradicate all *T. gondii* cysts from mouse brains and does not reliably prevent Toxoplasmosis relapse in AIDS patients and (Araujo, Huskinson, and Remington 1991; Kovacs 1992; Ferguson et al. 1994; Katlama, Mouthon, et al. 1996). Underlying reasons for this discrepancy need to be established but may include insufficient bioavailability. Quinolones are known to be poorly soluble in aqueous environments and the predicted permeability of the blood-brain barriers to either ATQ, BPQ and HDQ is low, suggesting that insufficient exposure to the drug may play a role in treatment failure. Indeed, BPQ treatment of mice that were experimentally infected with related parasite *Neospora caninum* did target parasites in muscle but not brain tissue (Müller et al. 2015). A similar conjecture arose when comparing to endochin-like quinolones where favorable pharmacokinetics of the variant of lower intrinsic potency likely conferred higher in vivo efficacy against cysts (Doggett et al. 2012).

Together, our data show the importance of the bc1-complex for the viability of bradyzoites and encourage the pursuit of bc1-inhibitors as candidates for eradicating toxoplasmosis treatments. Both, efforts to develop multi-site-directed inhibitors (Doggett et al. 2020; Alday, Nilsen, and Doggett 2022) and re-purposing of respective drugs are promising avenues. However, our data also underline the importance of favorable pharmacokinetics to ensure passage through the blood-brain barrier and the cyst wall.

The paper explained

Problem

The persisting bradyzoite stage of the zoonotic parasite *Toxoplasma gondii* is responsible for the chronic and reactivating infections as well as the transmission between intermediate hosts, including humans. To date, no medication effectively eradicates *T. gondii* cysts from infected individuals. Hence the dormant stage of these parasites represents an adamant obstacle for the disease burden of Toxoplasmosis. The current front-line treatment, the antifolate combination pyrimethamine - sulfadiazine targets the tachyzoite form of the parasite but can cause adverse side-effects due to their interference with host DNA synthesis that frequently leads to the discontinuation of the treatment. A less toxic alternative is atovaquone that targets the parasite cytochrome bc1-complex. However, these drugs, including promising candidates such as endochin-like quinolones, only reduce but do not eradicate encysted bradyzoites from brains of infected mice nor entirely prevent toxoplasmic encephalitis relapse in patients. Hence, the suitability of the folate pathway and the mitochondrial bc1 complex as a target structure for cidal drugs against bradyzoites remains unclear.

Results

400 compounds of Pathogen Box were tested in vitro against both stages of *T. gondii*, including pan-drug tolerant in vitro bradyzoites. We identified 14 inhibitors that were dually active without harming the host cells. In order to explore their modes of action, the metabolic response of the parasite to 6 MMV compounds was investigated. As a result, we confirmed the bc1-complex in mitochondrial electron transport as a valid target in both tachyzoites and otherwise drug tolerant in vitro bradyzoites. Other dually active compounds inhibit DHFR and DXR enzymes in other organisms.

Impact

The findings of this study direct the development of treatments of acute and chronic toxoplasmosis, by strongly suggesting the requirement of a functional bc1-complex in bradyzoites. This first application of our novel in vitro model for pan-drug tolerant bradyzoites aids to the delineation of underlying causes of treatment failures such as parasitic drug tolerance or pharmacokinetic insufficiencies.

Figures

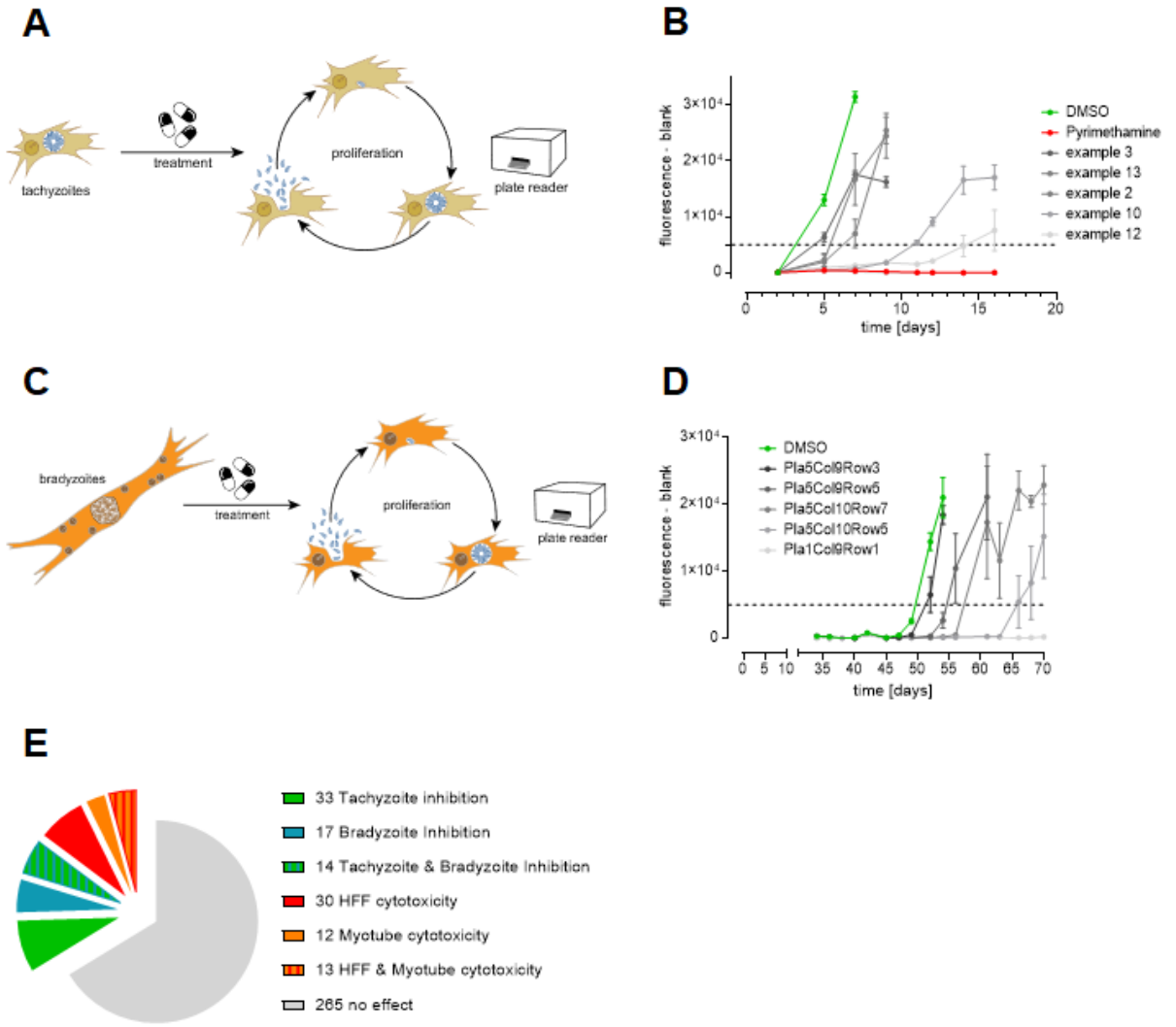

Figure 1: An in vitro screen reveals tachy- and bradyzoidal properties of the MMV Pathogen Box compounds.

(A) Experimental scheme of the MMV compound screen on *Toxoplasma gondii* tachyzoites in human foreskin fibroblast cells (B) Growth curves of tachyzoites treated with 10µM of each MMV compound for 7 days (shades of grey), a solvent control (green), and an inhibition control (red) (C) Experimental scheme of the MMV compound screen on bradyzoites matured in myotubes (D) Growth curves of bradyzoites treated with 10µM of each compound (shades of grey) or a solvent control (green) for 7 days, followed by a tachyzoite regrowth phase (E) Pie chart displaying the number of Pathogen Box compounds and their effects on our in vitro cultures

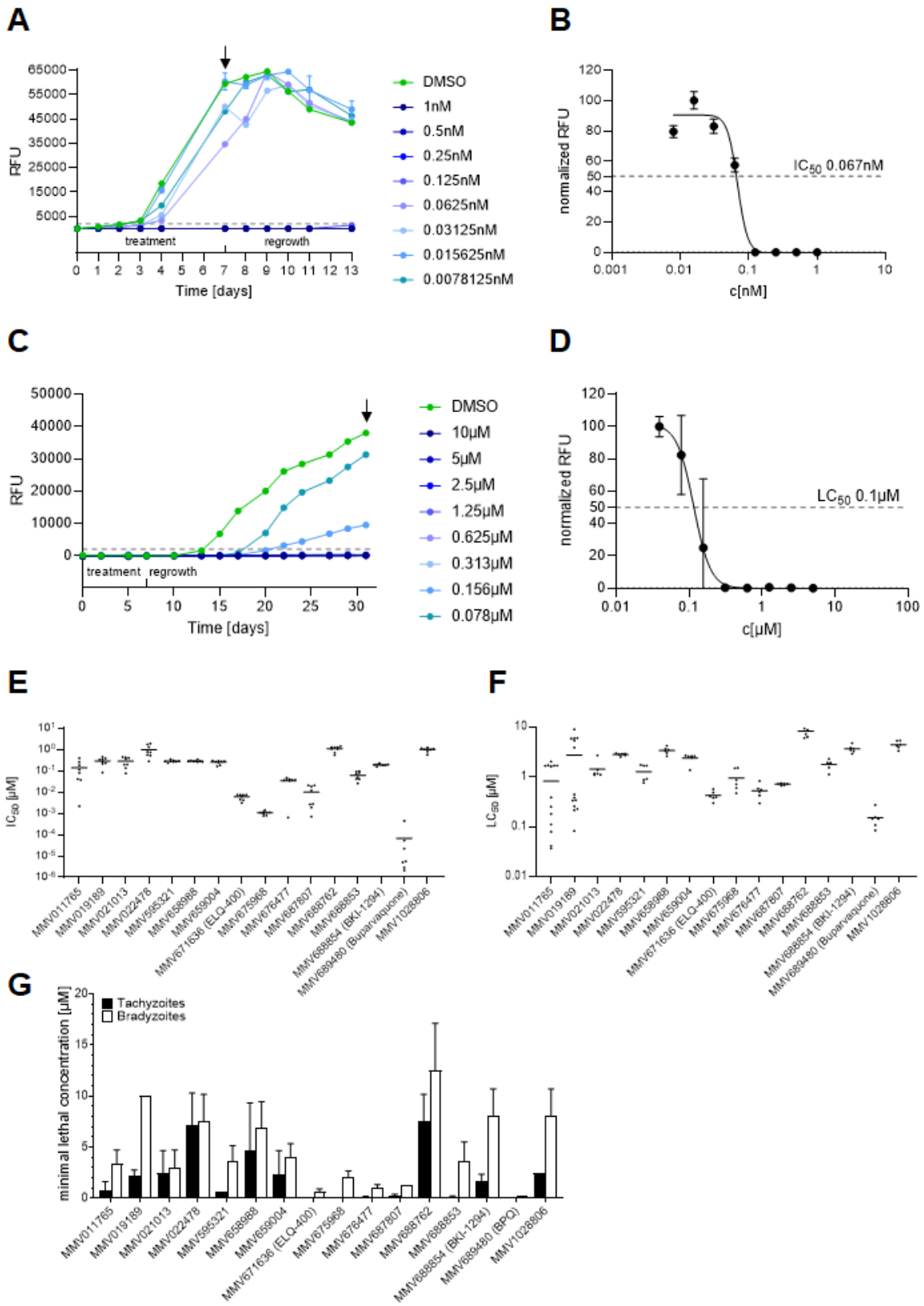

Figure 2: Confirmed Pathogen Box compounds that target both tachyzoites and mature bradyzoites.

(A) shows the growth curve of MMV689480 (Buparvaquone), one of the 16 dually active compounds, in a tachyzoite growth assay (n=8). The infected cultures were treated for 7 days and regrowth in absence of the inhibitor was observed for another week. Depending on the

development of the DMSO control, the half-maximal inhibitory concentration (IC_{50}) was determined at either day 4 or 7 (arrow). (B) shown is the respective data plotted as relative fluorescence units depending on the concentration at day 7. (C) With 4 weeks old, mature bradyzoite cultures (n=6) , the half-maximal lethal concentration (LC_{50}) was determined at the time point which ideally reflected the dose-response curve (in the case of Buparvaquone at day 31; arrow). (D) The LC_{50} of Buparvaquone on encysted bradyzoites determined at day 31. All IC_{50} and LC_{50} of dually active compounds are summarized in graph (E) for tachyzoite and (F) for bradyzoite cultures. (G) Comparison of the minimal lethal concentration of each compound on tachyzoites and bradyzoites.

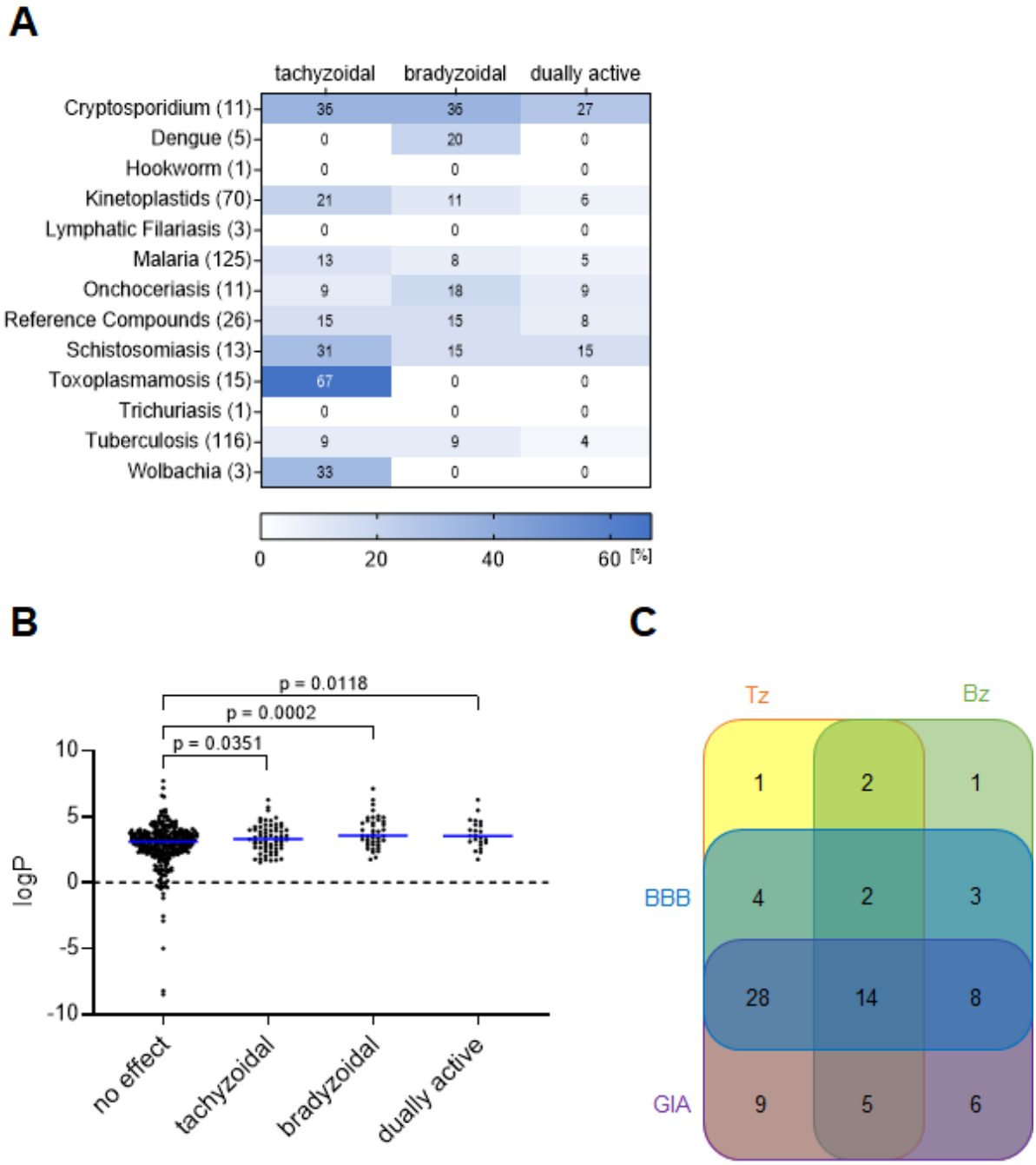

Figure 3: Properties of dually active screening hits.
(A) Table showing the relative amount of tachyzocidal, bradyzoidal and dually-active compounds per originally indicated target species. E.g. 11 compounds were indicated by MMV to be active against Cryptosporidium and 36% and 27% of these are bradyzoidal and dually active, whereas 67% of the 15 compounds indicated as active against Toxoplasmosis possessed activity against tachyzoites but none was active against against bradyzoites. (B) Estimated lipophilicity approximated by predicted partition coefficient suggest that active compounds generally exhibit an increased lipophilicity compared to inactive compounds and that bradyzoidal compounds are more lipophilic than tachyzocidal compounds. (C) A Venn diagram showing intersections of tachy- and bradyzoidal compounds as well as their predicted gastrointestinal absorption capability (GIA) and blood brain barrier (bbb) permeability.

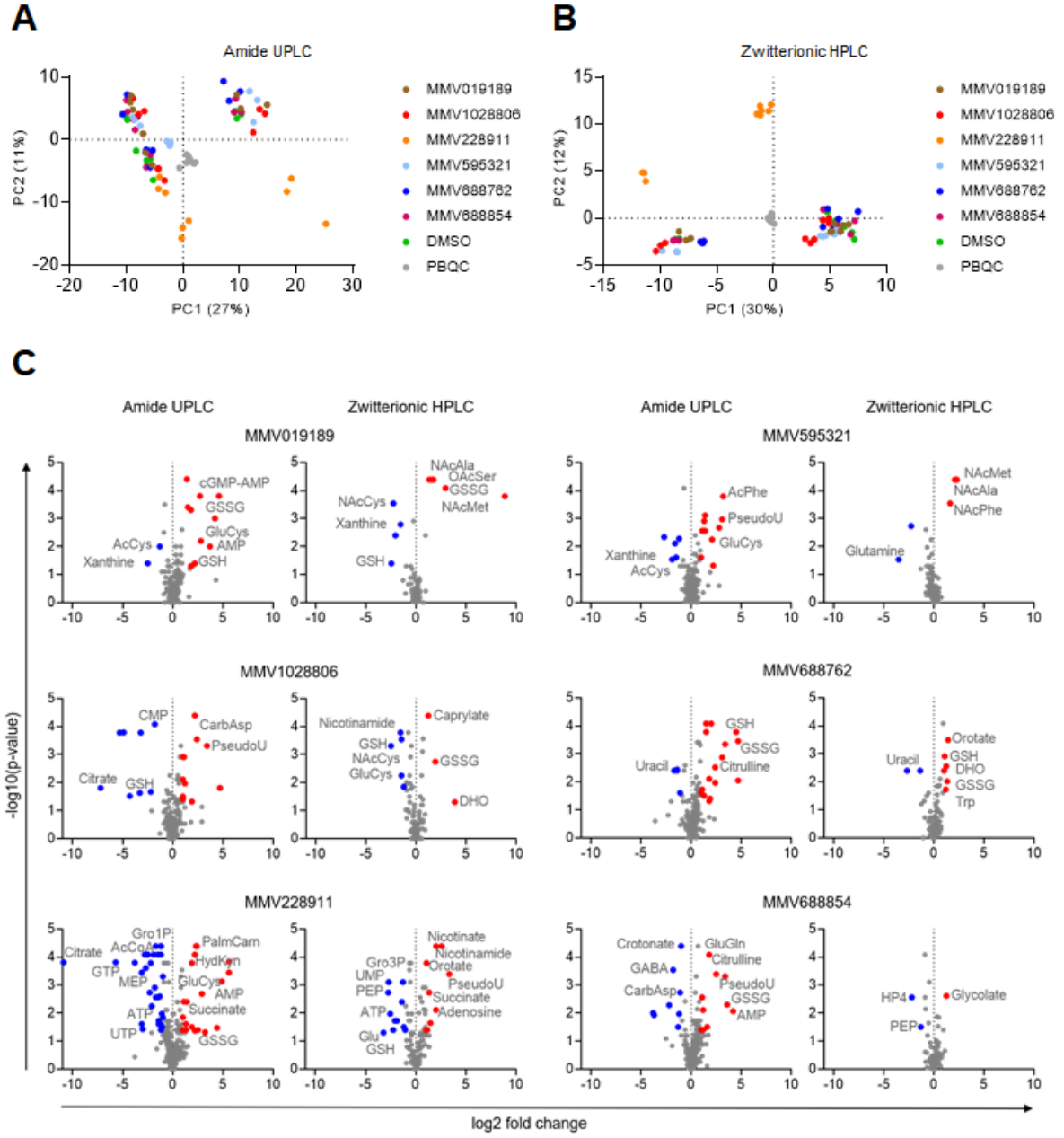

Figure 4: Untargeted metabolomics of tachyzoites treated with 6 screening hits effective against both stages of *T. gondii*.

(A) Principal component analysis of metabolites from extracellular tachyzoites that were treated with indicated MMV compounds. Metabolites were separted using BEH-Amide column -HILIC chromatography and detected by mass spectrometry. (B) The same metabolite extracts have been re-analysed using pHILIC-column HILIC chromatograophy for separation instead. (C) Volcano plots showing the parasitic, intracellular metabolic phenotype caused by MMV Pathogen Box compounds that inhibited tachyzoites and bradyzoites during the screen. The metabolome was measured with two columns of complementary chemistries to enhance metabolite coverage. Blue dots indicate metabolites which were significantly reduced compared to DMSO treated parasites and red dots indicate significantly accumulated metabolites ($p < 0.05$, log2 fold change <-1 or > 1, 3x biological replicates with 3x technical replicates each, n = 9). Abrreviations: AcCoA = Acetyl-CoA, AcCys = Acetylcysteine, AcPhe =

Acetylphenylalanine, AMP = Adenosinemonophosphate, ATP = Adenosinetriphosphate, CarbAsp = Carbamoylaspartate, cGMP-AMP = cyclic Guanosinemonophosphate-adenosinemonophosphate, CMP = Cytosinemonophosphate, DHO = Dihydroorotate, GABA = gamma-Aminobutyratic acid, GluCys = Glutamylcysteine, GluGln = Glutamylglutamine, Gro1P = Glyceraldehyde 1-phosphate, Gro3P = Glyceraldehyde 3-phosphate, GSH = Glutathione oxidized, GSSG = Glutathione reduced, GTP = Guanosinetriphosphate, HP4 = forth chromatographic peak of 260.02972, HydKyn = Hydroxylkynurenine, MEP = 2-C-Methyl-D-erythritol 4-phosphate, NAcAla = N-Acetylalanine, NAcCys = N-Acetylcysteine, NAcMet = N-Acetylmethionine, NAcPhe = N-Acetylphenylalanine, OAcSer = O-Acetylserine, PalmCarn = Palmitoylcarnitine, PEP = Phosphoenolpyruvate, PseudoU = Pseudouridine, Trp = Tryptophane, UMP = Uridinemonophosphate, UTP = Uridinetriphosphate

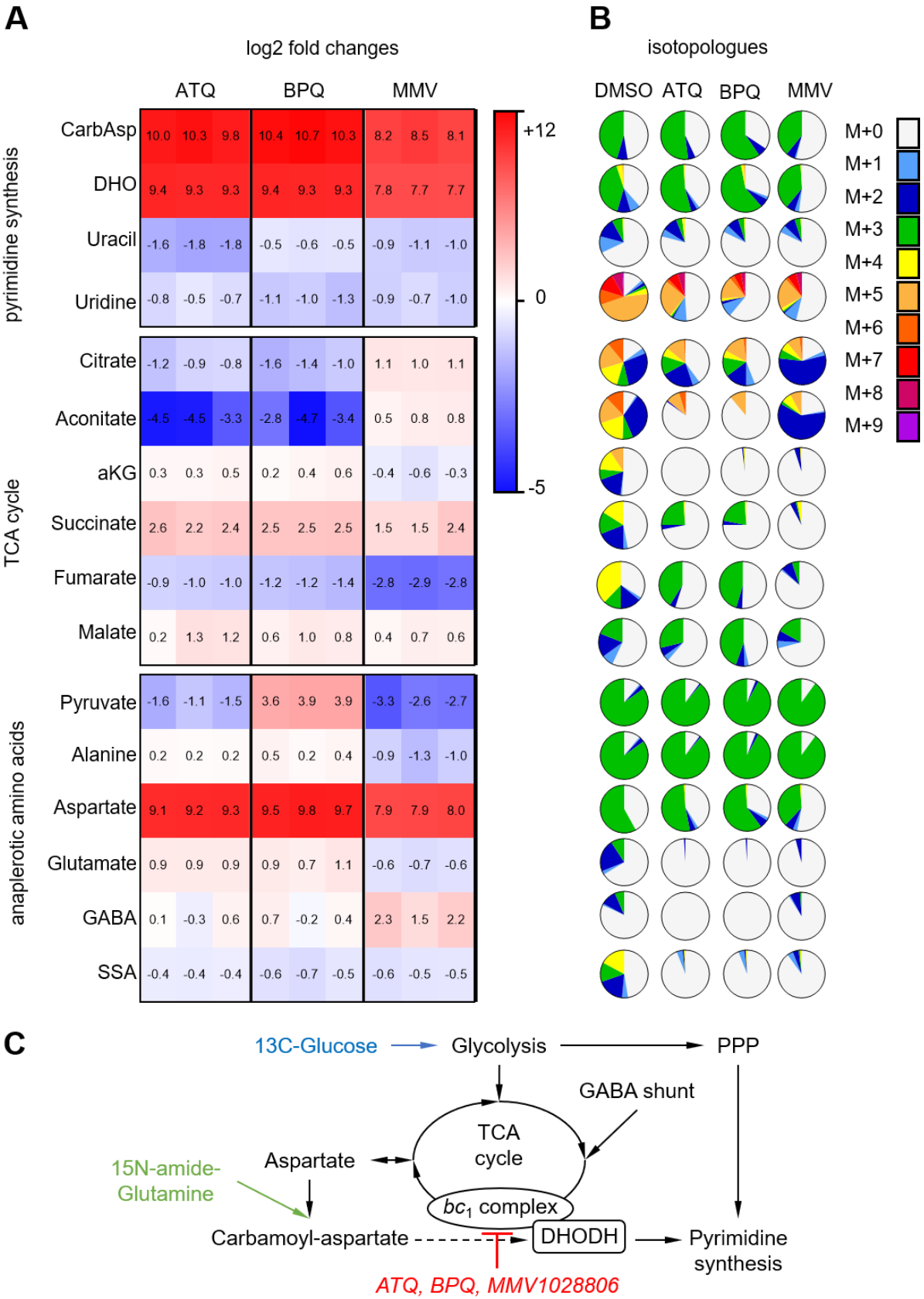
A
log2 fold changes
ATQ
BPQ
MMV
pyrimidine synthesis
CarbAsp 10.0 10.3 9.8 10.4 10.7 10.3 8.2 8.5 8.1
DHO 9.4 9.3 9.3 9.4 9.3 9.3 7.8 7.7 7.7
Uracil -1.6 -1.8 -1.8 -0.5 -0.6 -0.5 -0.9 -1.1 -1.0
Uridine -0.8 -0.5 -0.7 -1.1 -1.0 -1.3 -0.9 -0.7 -1.0
TCA cycle
Citrate -1.2 -0.9 -0.8 -1.6 -1.4 -1.0 1.1 1.0 1.1
Aconitate -4.5 -4.5 -3.3 -2.8 -4.7 -3.4 0.5 0.8 0.8
aKG 0.3 0.3 0.5 0.2 0.4 0.6 -0.4 -0.6 -0.3
Succinate 2.6 2.2 2.4 2.5 2.5 2.5 1.5 1.5 2.4
Fumarate -0.9 -1.0 -1.0 -1.2 -1.2 -1.4 -2.8 -2.9 -2.8
Malate 0.2 1.3 1.2 0.6 1.0 0.8 0.4 0.7 0.6
anaplerotic amino acids
Pyruvate -1.6 -1.1 -1.5 3.6 3.9 3.9 -3.3 -2.6 -2.7
Alanine 0.2 0.2 0.2 0.5 0.2 0.4 -0.9 -1.3 -1.0
Aspartate 9.1 9.2 9.3 9.5 9.8 9.7 7.9 7.9 8.0
Glutamate 0.9 0.9 0.9 0.9 0.7 1.1 -0.6 -0.7 -0.6
GABA 0.1 -0.3 0.6 0.7 -0.2 0.4 2.3 1.5 2.2
SSA -0.4 -0.4 -0.4 -0.6 -0.7 -0.5 -0.6 -0.5 -0.5
+12
0
-5
B
isotopologues
DMSO ATQ BPQ MMV
M+0
M+1
M+2
M+3
M+4
M+5
M+6
M+7
M+8
M+9
C
13C-Glucose
Glycolysis
PPP
GABA shunt
TCA cycle
15N-amide-Glutamine
Aspartate
bc1 complex
Carbamoyl-aspartate
DHODH
Pyrimidine synthesis
ATQ, BPQ, MMV1028806

Figure 5: The metabolic response to electron transport chain inhibitors and MMV1028806.

Intracellular tachyzoites were labeled with U-^{13}C-glucose and treated with atovaquone, buparvaquone and MMV1028806 for 3 h. Showing (A) the log2-fold changes to a DMSO treated sample of ETC related metabolites and (B) their average isotopologue distribution. Abbreviations: ATQ = atovaquone, BPQ = buparvaquone, aKG = alpha-Ketoglutarate, DHO = Dihydroorotate, GABA = gamma-Aminobutyrate, SSA = Succinic semialdehyde (C) Scheme of the affected pathways upon bc1 complex inhibition

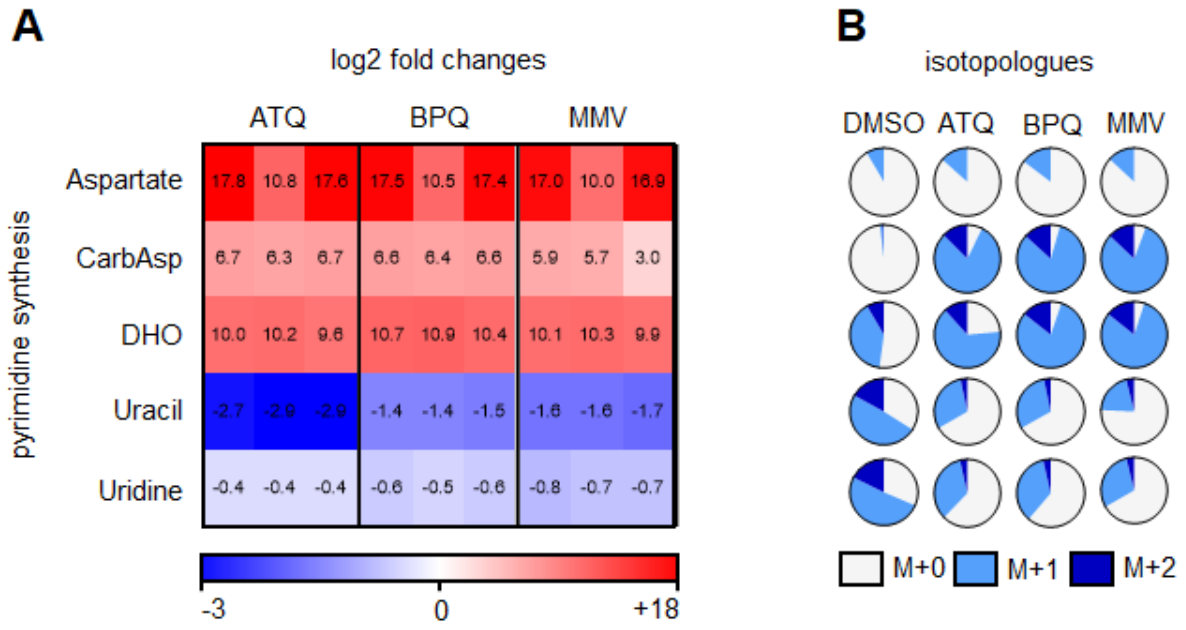

Figure 6: ^{15}N-amide-glutamine labeling of intracellular parasites treated with electron transport chain inhibitors.

Infected monolayers were treated with electron transport chain inhibitors atovaquone (ATQ), Burparvaquone (BPQ), MMV1028806 or DMSO as solvent controls for three hours while simultaneously glutamine was replaced by ^{15}N-amide-glutamine from the culture media. (A) Heatmap showing mean log2-fold changes between solvent controls and treated parasites as per LCMS analysis. Aspartate, carbamoyl-aspartate (CarbAsp) and dihydroorotate (DHO) accumulate upon all three treatments. (B) Pie charts showing isotopologue distribution of metabolites in the same experiment as in A. All three treatments decrease both M+1 and M+2 isotopologues while increasing labeling of CarbAsp and DHO.

A

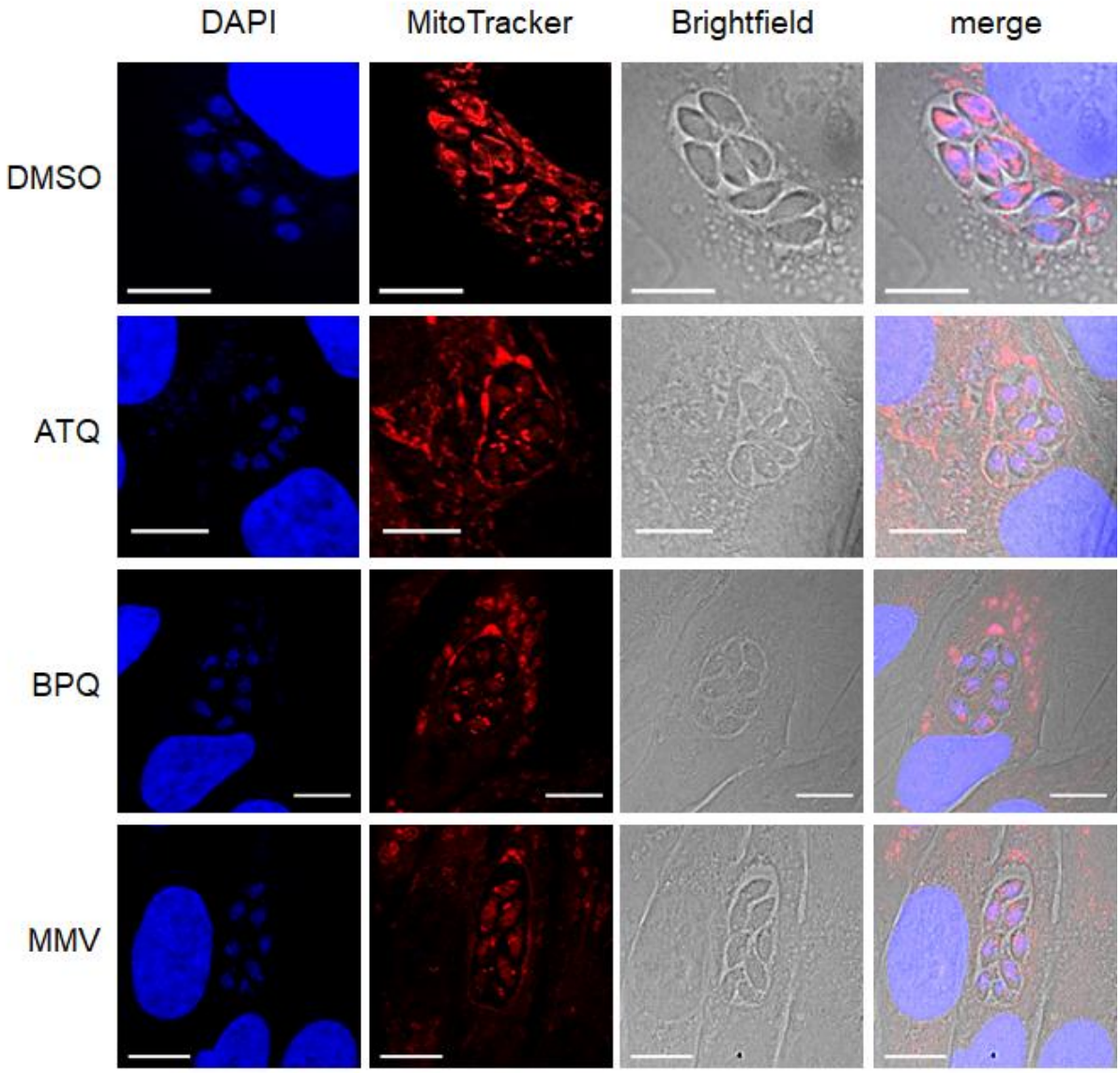
DAPI
MitoTracker
Brightfield
merge
DMSO
ATQ
BPQ
MMV

B

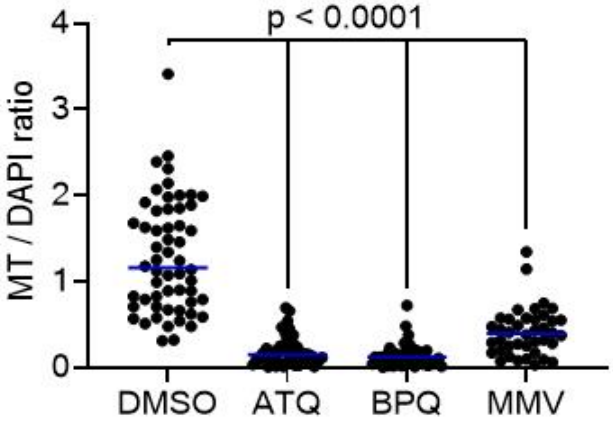
p < 0.0001
MT / DAPI ratio
4
3
2
1
0
DMSO
ATQ
BPQ
MMV

Figure 7: An electron-potential dependent mitochondrial stain shows depleted mitochondrial electron potential in atovaquone (ATQ), buparvaquone (BPQ) and MMV1028806 treated tachyzoites.

(A) HFF cells were infected with tachyzoites and treated with DMSO, atovaquone, buparvaquone and MMV1028806 for 24 h, and mitochondria were stained with mitotracker (red) and DNA was stained with DAPI (blue). scale bar = 10 µm. (B) The ratios of fluorescence intensities between mitotracker (MT) and DAPI dyes were calculated per vacuole (DMSO n = 56, ATQ n = 45, BPQ n = 49, MMV1028806 n = 40; Blue lines represent the median, two-sided Mann-Whitney test).

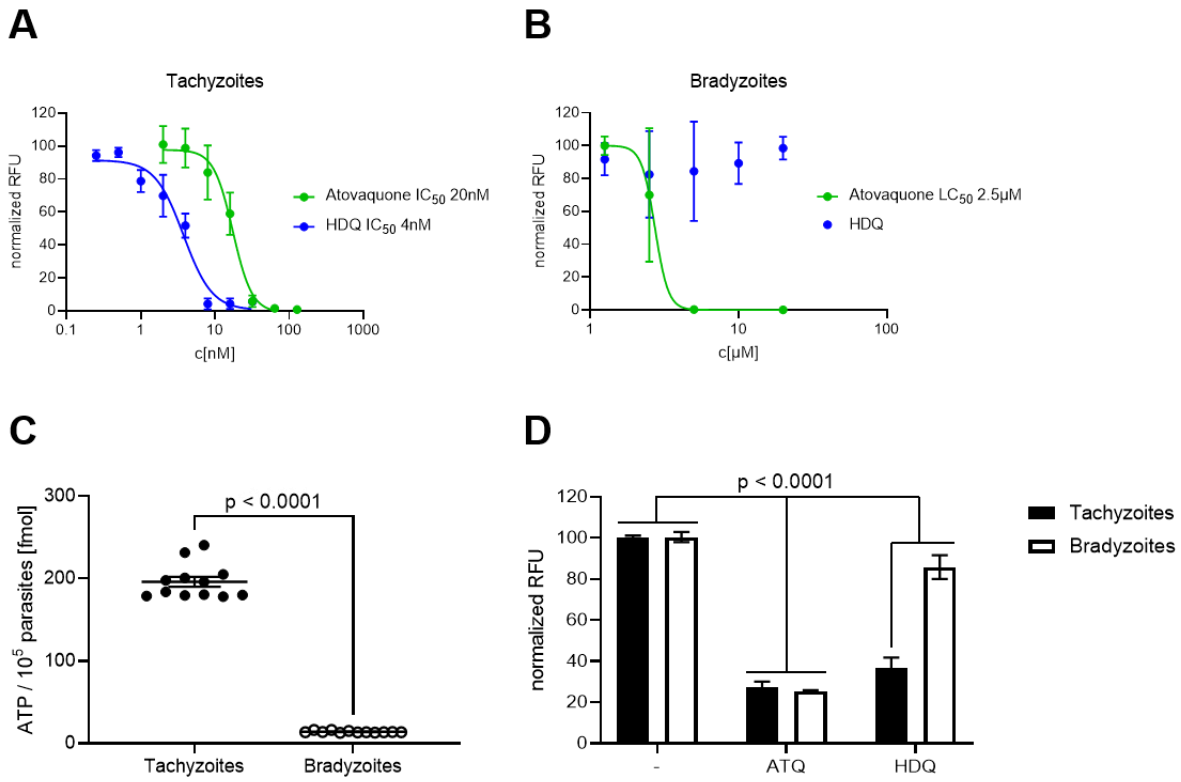

Figure 8: Differential efficacy and ATP depletion by atovaquone and HDQ in tachyzoites and bradyzoites

Atovaquone and HDQ were tested against *T. gondii* Prugeniaud parasites. (A) Showing the normalized half-maximal inhibitory concentration (IC_{50}) against tachyzoites in fibroblasts at day 4, n=8. (B) 4 week-old bradyzoites were treated for a week with Atovaquone or HDQ. Cultures were observed for tachyzoite re-growth for three weeks. The half-maximal lethal concentration (LC_{50}) was determined at the time point which ideally reflected the dose-response curve, in this case day 14, n=6. 10^5 tachyzoites and bradyzoites were lysed and the ATP concentration was determined with an enzymatic luciferase assay. (C) Showing the calculated concentration of ATP within an average parasite. Lines reflect the median, error bars represent SEM, significance test Mann-Whitney, n=12. (D) Parasites were treated with 1 µM Atovaquone or HDQ. The RFUs were normalized to the untreated control of either the tachyzoite or bradyzoite dataset. Bars reflect the mean, error bars represent SEM, significance test two-way ANOVA with Tukey correction, n=6.

Acknowledgements / Funding

We thank Naohiro Hashimoto for sharing the KD3 cells, Frank Seeber for the *T. gondii* strains and the Medicine for Malaria Venture for the Pathogen Box.

MB, DM, EH, EP are funded by the Federal Ministry of Education and Research (BMBF) under project number 01KI1715 as part of the "Research Network Zoonotic Infectious Diseases".

Supplements

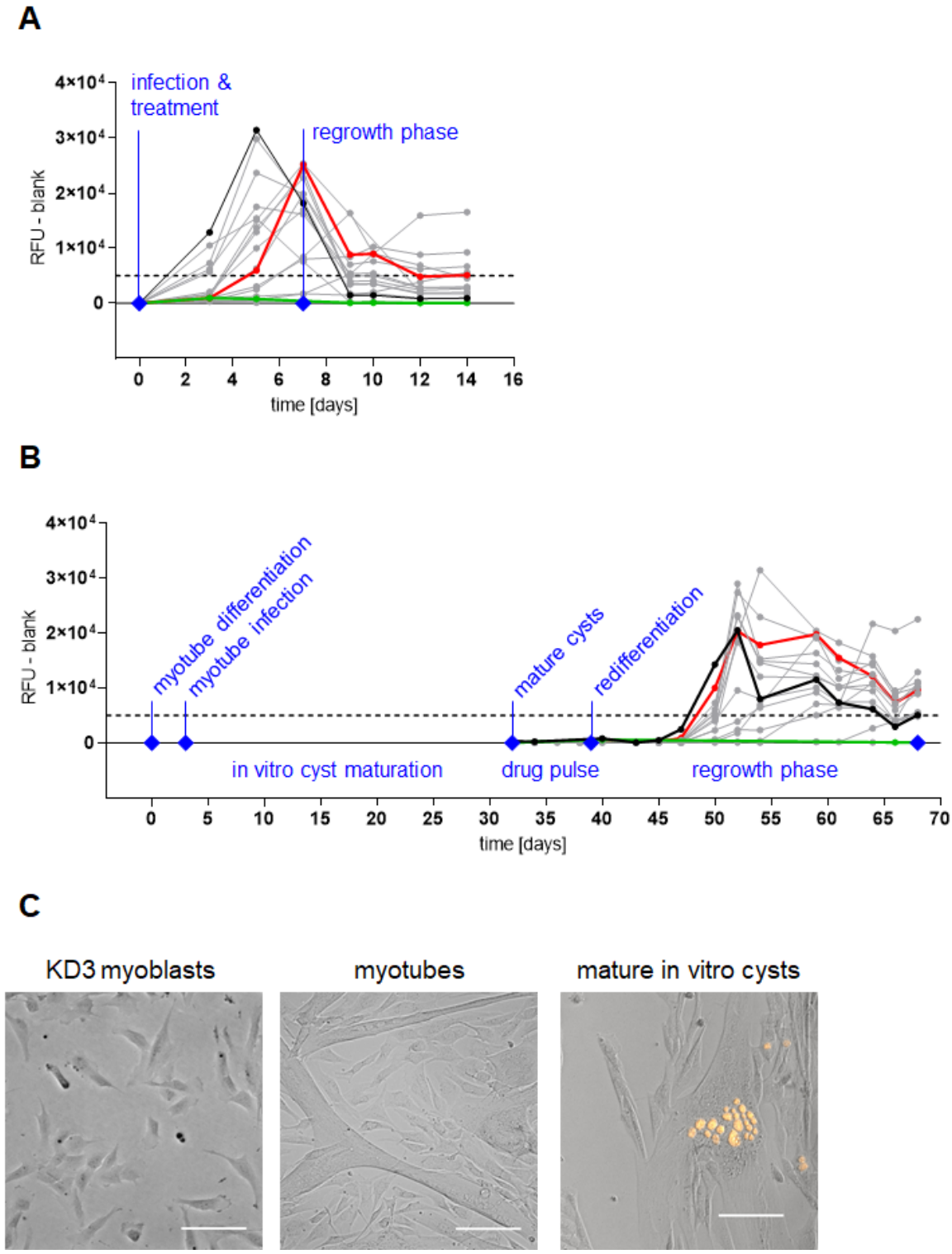

Figure S1: Longitudinal Screening Procedure

All 400 compounds of the MMV Pathogen Box were screened against (A) tachyzoites (n = 4) and (B) in vitro tissue cysts (n = 3). Plotted fluorescence values were background-subtracted and reflect the abundance of parasites per treatment over time (black line = solvent control, green line = inhibitory compound, red line = ineffective compound, dashed line = growth threshold). (C) KD3 myoblasts were differentiated to myotubes and infected with PruTom which matured to tissue cysts within 4 weeks (scale bar = 100 µM).

Compound	Tachyzoite IC_{50} [µM] Mean ± SEM	Bradyzoite LC_{50} [µM] Mean ± SEM
MMV011765	0.14 ± 0.05	0.8 ± 0.2
MMV019189	0.28 ± 0.04	2.7 ± 0.8
MMV021013	0.28 ± 0.05	1.4 ± 0.3
MMV022478	1 ± 0.2	2.79 ± 0.07
MMV595321	0.28 ± 0.01	1.3 ± 0.2
MMV658988	0.28 ± 0.01	3.4 ± 0.2
MMV659004	0.25 ± 0.02	2.4 ± 0.2
MMV671636 (ELQ-400)	0.0059 ± 0.0006	0.42 ± 0.04
MMV675968	0.00105 ± 0.00007	0.9 ± 0.2
MMV676477	0.034 ± 0.005	0.53 ± 0.07
MMV687807	0.01 ± 0.003	0.71 ± 0.01
MMV688762	1.1 ± 0.1	8.2 ± 0.9
MMV688853	0.061 ± 0.009	1.8 ± 0.2
MMV688854 (BKI-1294)	0.191 ± 0.007	3.6 ± 0.3
MMV689480 (BPQ)	0.00007 ± 0.00006	0.15 ± 0.03
MMV1028806	0.98 ± 0.07	4.4 ± 0.3

Figure S2: 14 dually active compounds and their effective concentrations.

The calculated IC_{50}s and LC_{50}s of the dually active compounds from figure 2 are summarized in this table. The tachyzoite IC_{50}s represent 8 replicates, the bradyzoidal one were generated from 6 replicates.

	untreated			ATQ			BPQ			MMV			
Glutamine	87	84	87	91	91	91	93	94	93	93	92	92	amino acids & amino acid derivates
Glutamate	49	48	48	15	16	15	15	15	15	35	35	35	
GABA	36	38	39	14	13	13	17	17	15	29	32	29	
Alanine	40	37	38	10	9	9	8	9	8	23	28	22	
Aspartate	7	9	9	12	15	14	14	15	15	12	13	14	
Proline	10	11	11	4	4	5	4	4	5	6	5	5	
Oxoproline	17	12	17	2	2	2	2	1	2	10	11	10	
NAcAspGlu	53	42	44	4	3	7	1	7	6	36	33	34	
Leucine	1	1	0	2	2	1	1	1	1	2	1	1	
Isoleucine	2	1	2	3	3	4	2	2	2	2	2	3	
Glycine	3	2	2	0	0	1	1	0	0	1	0	1	
CarbAsp	2	1	25	93	92	93	95	96	96	94	94	94	pyrimidine metabolism
Dihydroorotate	47	49	42	94	93	93	96	96	96	95	95	95	
Uracil	66	67	65	33	33	33	33	34	33	24	24	24	
Uridine	69	69	68	37	38	38	40	38	39	33	33	33	
UDPGlucNAc	96	98	97	95	96	97	96	97	97	96	96	96	
Desoxyuridine	48	47	47	17	17	16	17	17	16	35	37	9	
Cytosine	78	75	80	76	77	77	76	76	75	78	78	78	
Cytidine	83	83	83	74	74	76	76	76	75	78	77	78	
Desoxycytidine	18	14	14	21	21	20	19	15	28	18	19	17	
Xanthosine	54	56	57	57	57	58	49	48	46	56	55	56	purine metabolism
Inosine	60	60	60	70	68	67	61	58	60	62	62	58	
Hypoxanthine	59	56	59	68	67	69	62	62	62	62	62	62	
Guanosine	85	86	86	70	70	70	66	66	66	76	76	75	
Guanine	89	84	86	60	61	62	64	65	65	77	76	77	
cAMP	59	59	60	69	68	69	60	58	60	63	62	64	
AMP	52	55	55	70	58	77	54	48	51	55	59	55	
Adenine	60	55	63	63	61	61	56	56	54	59	63	60	
Adenosine	65	65	65	69	69	69	62	62	61	65	65	64	
dInosine	54	52	47	32	34	32	43	42	42	40	40	39	
Nicotinamide	71	72	77	33	28	30	29	24	27	54	56	51	misc.
NAD+	96	95	95	70	72	69	67	68	69	79	80	80	
GlucNAcP	90	86	89	78	78	76	85	81	77	79	81	83	

0 % 50 % 100 %

Figure S3: Intracellular tachyzoites exhibit differential ^{15}N incorporation after treatment with ETC inhibitors.

RH-KU80 were treated with atovaquone, buparvaquone and MMV1028806, labeled with ^{15}N-amide-L-glutamine for 3h, followed by their isolation from the HFF cells. The heatmap shows the overall isotopic labeling (100-"M+0") of each replicate.

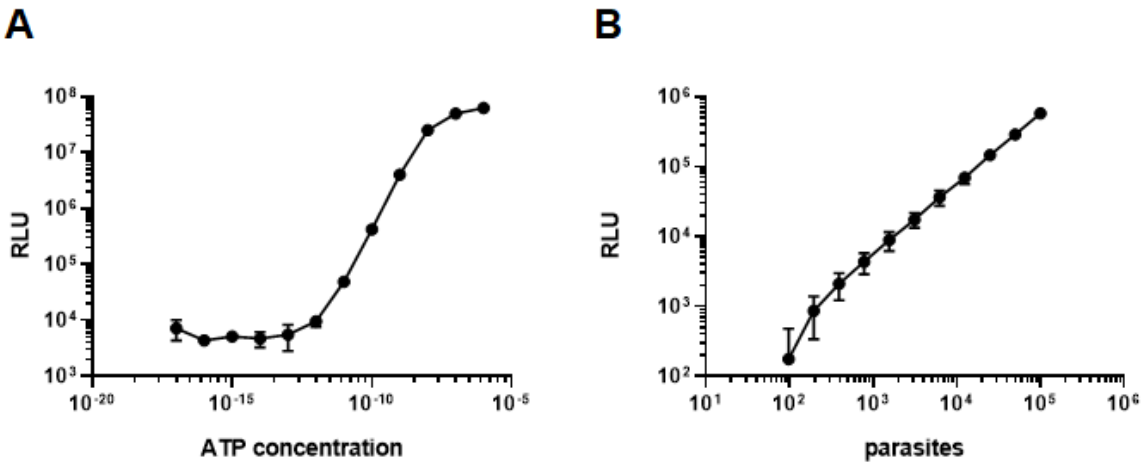

Figure S4: Luminescence-based ATP assay

(A) The linear response of the BacTiter-Glo™ assay has a certain range, depending on the ATP concentration of the sample. The assay is reliable between 100fM and 1nM ATP. (B) Increasing numbers of freshly isolated parasites were analysed to determine a minimal parasite density necessary for steady readouts. 10^5 parasites per sample were both manageable and accurate.

References

Alday, P. Holland, and Joseph Stone Doggett. 2017. “Drugs in Development for Toxoplasmosis: Advances, Challenges, and Current Status.” *Drug Design, Development and Therapy* 11 (January): 273–93. https://doi.org/10.2147/DDDT.S60973.

Alday, P. Holland, Aaron Nilsen, and J. Stone Doggett. 2022. “Structure-Activity Relationships of Toxoplasma Gondii Cytochrome bc1 Inhibitors.” *Expert Opinion on Drug Discovery* 17 (9): 997–1011. https://doi.org/10.1080/17460441.2022.2096588.

Allman, Erik L., Heather J. Painter, Jasmeet Samra, Manuela Carrasquilla, and Manuel Llinás. 2016. “Metabolomic Profiling of the Malaria Box Reveals Antimalarial Target Pathways.” *Antimicrobial Agents and Chemotherapy* 60 (11): 6635–49. https://doi.org/10.1128/AAC.01224-16.

Anglada-Girotto, Miquel, Gabriel Handschin, Karin Ortmayr, Adrian I. Campos, Ludovic Gillet, Pablo Manfredi, Claire V. Mulholland, et al. 2022. “Combining CRISPRi and Metabolomics for Functional Annotation of Compound Libraries.” *Nature Chemical Biology* 18 (5): 482–91. https://doi.org/10.1038/s41589-022-00970-3.

Antonova-Koch, Yevgeniya, Stephan Meister, Matthew Abraham, Madeline R. Luth, Sabine Ottilie, Amanda K. Lukens, Tomoyo Sakata-Kato, et al. 2018. “Open-Source Discovery of Chemical Leads for next-Generation Chemoprotective Antimalarials.” *Science* 362 (6419). https://doi.org/10.1126/science.aat9446.

Araujo, F. G., J. Huskinson, and J. S. Remington. 1991. “Remarkable in Vitro and in Vivo Activities of the Hydroxynaphthoquinone 566C80 against Tachyzoites and Tissue Cysts of Toxoplasma Gondii.” *Antimicrobial Agents and Chemotherapy* 35 (2): 293–99. https://doi.org/10.1128/AAC.35.2.293.

Asai, Takashi, William J. O’Sullivan, Masashi Kobayashi, Annette M. Gero, Muneo Yokogawa, and Masamiti Tatibana. 1983. “Enzymes of the de Novo Pyrimidine Biosynthetic Pathway in Toxoplasma Gondii.” *Molecular and Biochemical Parasitology* 7 (2): 89–100. https://doi.org/10.1016/0166-6851(83)90037-3.

Bajohr, Lara Liv, Ling Ma, Christian Platte, Oliver Liesenfeld, Lutz F. Tietze, Uwe Gross, and Wolfgang Bohne. 2010. “In Vitro and in Vivo Activities of 1-Hydroxy-2-Alkyl-4(1H)quinolone Derivatives against Toxoplasma Gondii.” *Antimicrobial Agents and Chemotherapy* 54 (1): 517–21. https://doi.org/10.1128/AAC.01001-09.

Baumeister, Stefan, Jochen Wiesner, Armin Reichenberg, Martin Hintz, Sven Bietz, Omar S. Harb, David S. Roos, et al. 2011. “Fosmidomycin Uptake into Plasmodium and Babesia-Infected Erythrocytes Is Facilitated by Parasite-Induced New Permeability Pathways.” *PloS One* 6 (5): e19334. https://doi.org/10.1371/journal.pone.0019334.

Berry, Sarah L., Hamza Hameed, Anna Thomason, Marissa L. Maciej-Hulme, Somaia Saif Abou-Akkada, Paul Horrocks, and Helen P. Price. 2018. “Development of NanoLuc-PEST Expressing Leishmania Mexicana as a New Drug Discovery Tool for Axenic- and Intramacrophage-Based Assays.” *PLoS Neglected Tropical Diseases* 12 (7): e0006639. https://doi.org/10.1371/journal.pntd.0006639.

Borba-Santos, Luana Pereira, Taissa Vila, and Sonia Rozental. 2020. “Identification of Two Potential Inhibitors of Sporothrix Brasiliensis and Sporothrix Schenckii in the Pathogen Box Collection.” *PloS One* 15 (10): e0240658. https://doi.org/10.1371/journal.pone.0240658.

Campos, Adrian I., and Mattia Zampieri. 2019. “Metabolomics-Driven Exploration of the Chemical Drug Space to Predict Combination Antimicrobial Therapies.” *Molecular Cell* 74 (6): 1291–1303.e6. https://doi.org/10.1016/j.molcel.2019.04.001.

Cantillon, Daire, Aaron Goff, Stuart Taylor, Emad Salehi, Katy Fidler, Simon Stoneham, and Simon J. Waddell. 2022. “Searching for New Therapeutic Options for the Uncommon Pathogen Mycobacterium Chimaera: An Open Drug Discovery Approach.” *The Lancet. Microbe* 3 (5): e382–91. https://doi.org/10.1016/S2666-5247(21)00326-8.

Caro, Pilar, Amar U. Kishan, Erik Norberg, Illana A. Stanley, Bjoern Chapuy, Scott B. Ficarro,

Klaudia Polak, et al. 2012. “Metabolic Signatures Uncover Distinct Targets in Molecular Subsets of Diffuse Large B Cell Lymphoma.” *Cancer Cell* 22 (4): 547–60. https://doi.org/10.1016/j.ccr.2012.08.014.

Cerneckis, Jonas, Qi Cui, Chuan He, Chengqi Yi, and Yanhong Shi. 2022. “Decoding Pseudouridine: An Emerging Target for Therapeutic Development.” *Trends in Pharmacological Sciences* 43 (6): 522–35. https://doi.org/10.1016/j.tips.2022.03.008.

Christiansen, Céline, Deborah Maus, Ellen Hoppenz, Mateo Murillo-León, Tobias Hoffmann, Jana Scholz, Florian Melerowicz, Tobias Steinfeldt, Frank Seeber, and Martin Blume. 2022. “In Vitro Maturation of Toxoplasma Gondii Bradyzoites in Human Myotubes and Their Metabolomic Characterization.” *Nature Communications* 13 (1): 1168. https://doi.org/10.1038/s41467-022-28730-w.

Creek, Darren J., Hwa H. Chua, Simon A. Cobbold, Brunda Nijagal, James I. MacRae, Benjamin K. Dickerman, Paul R. Gilson, Stuart A. Ralph, and Malcolm J. McConville. 2016. “Metabolomics-Based Screening of the Malaria Box Reveals Both Novel and Established Mechanisms of Action.” *Antimicrobial Agents and Chemotherapy* 60 (11): 6650–63. https://doi.org/10.1128/AAC.01226-16.

Daina, Antoine, Olivier Michielin, and Vincent Zoete. 2017. “SwissADME: A Free Web Tool to Evaluate Pharmacokinetics, Drug-Likeness and Medicinal Chemistry Friendliness of Small Molecules.” *Scientific Reports* 7 (March): 42717. https://doi.org/10.1038/srep42717.

Davis, D. R. 1995. “Stabilization of RNA Stacking by Pseudouridine.” *Nucleic Acids Research* 23 (24): 5020–26. https://doi.org/10.1093/nar/23.24.5020.

DeRocher, A., C. B. Hagen, J. E. Froehlich, J. E. Feagin, and M. Parsons. 2000. “Analysis of Targeting Sequences Demonstrates That Trafficking to the Toxoplasma Gondii Plastid Branches off the Secretory System.” *Journal of Cell Science* 113 (Pt 22) (November): 3969–77. https://doi.org/10.1242/jcs.113.22.3969.

Doggett, J. Stone, Aaron Nilsen, Isaac Forquer, Keith W. Wegmann, Lorraine Jones-Brando, Robert H. Yolken, Claudia Bordón, et al. 2012. “Endochin-like Quinolones Are Highly Efficacious against Acute and Latent Experimental Toxoplasmosis.” *Proceedings of the National Academy of Sciences of the United States of America* 109 (39): 15936–41. https://doi.org/10.1073/pnas.1208069109.

Doggett, J. Stone, Kayode K. Ojo, Erkang Fan, Dustin J. Maly, and Wesley C. Van Voorhis. 2014. “Bumped Kinase Inhibitor 1294 Treats Established Toxoplasma Gondii Infection.” *Antimicrobial Agents and Chemotherapy* 58 (6): 3547–49. https://doi.org/10.1128/AAC.01823-13.

Doggett, J. Stone, Tracey Schultz, Alyssa J. Miller, Igor Bruzual, Sovitj Pou, Rolf Winter, Rozalia Dodean, et al. 2020. “Orally Bioavailable Endochin-Like Quinolone Carbonate Ester Prodrug Reduces Toxoplasma Gondii Brain Cysts.” *Antimicrobial Agents and Chemotherapy* 64 (9). https://doi.org/10.1128/AAC.00535-20.

Duffy, Sandra, Melissa L. Sykes, Amy J. Jones, Todd B. Shelper, Moana Simpson, Rebecca Lang, Sally-Ann Poulsen, Brad E. Sleebs, and Vicky M. Avery. 2017. “Screening the Medicines for Malaria Venture Pathogen Box across Multiple Pathogens Reclassifies Starting Points for Open-Source Drug Discovery.” *Antimicrobial Agents and Chemotherapy* 61 (9). https://doi.org/10.1128/AAC.00379-17.

Enshaeieh, Marjan, Geita Saadatnia, Jalal Babaie, Majid Golkar, Samira Choopani, and Mohammad Sayyah. 2021. “Valproic Acid Inhibits Chronic Toxoplasma Infection and Associated Brain Inflammation in Mice.” *Antimicrobial Agents and Chemotherapy* 65 (10): e0100321. https://doi.org/10.1128/AAC.01003-21.

Ferguson, D. J., J. Huskinson-Mark, F. G. Araujo, and J. S. Remington. 1994. “An Ultrastructural Study of the Effect of Treatment with Atovaquone in Brains of Mice Chronically Infected with the ME49 Strain of Toxoplasma Gondii.” *International Journal of Experimental Pathology* 75 (2): 111–16. https://www.ncbi.nlm.nih.gov/pubmed/8199003.

Fu, Yong, Kevin M. Brown, Nathaniel G. Jones, Silvia Nj Moreno, and L. David Sibley. 2021. “Toxoplasma Bradyzoites Exhibit Physiological Plasticity of Calcium and Energy Stores Controlling Motility and Egress.” *eLife* 10 (December).

https://doi.org/10.7554/eLife.73011.
Guggisberg, Ann M., Jooyoung Park, Rachel L. Edwards, Megan L. Kelly, Dana M. Hodge, Niraj H. Tolia, and Audrey R. Odom. 2014. “A Sugar Phosphatase Regulates the Methylerythritol Phosphate (MEP) Pathway in Malaria Parasites.” *Nature Communications* 5 (1): 4467. https://www.nature.com/articles/ncomms5467.
Havelaar, Arie H., Martyn D. Kirk, Paul R. Torgerson, Herman J. Gibb, Tine Hald, Robin J. Lake, Nicolas Praet, et al. 2015. “World Health Organization Global Estimates and Regional Comparisons of the Burden of Foodborne Disease in 2010.” *PLoS Medicine* 12 (12): e1001923. https://doi.org/10.1371/journal.pmed.1001923.
Hayward, Jenni A., F. Victor Makota, Daniela Cihalova, Rachel A. Leonard, Esther Rajendran, Soraya M. Zwahlen, Laura Shuttleworth, et al. 2023. “A Screen of Drug-like Molecules Identifies Chemically Diverse Electron Transport Chain Inhibitors in Apicomplexan Parasites.” *PLoS Pathogens* 19 (7): e1011517. https://doi.org/10.1371/journal.ppat.1011517.
Hegewald, Jana, Uwe Gross, and Wolfgang Bohne. 2013. “Identification of Dihydroorotate Dehydrogenase as a Relevant Drug Target for 1-Hydroxyquinolones in Toxoplasma Gondii.” *Molecular and Biochemical Parasitology* 190 (1): 6–15. https://doi.org/10.1016/j.molbiopara.2013.05.008.
Hennessey, Kelly M., Ilse C. Rogiers, Han-Wei Shih, Matthew A. Hulverson, Ryan Choi, Molly C. McCloskey, Grant R. Whitman, et al. 2018. “Screening of the Pathogen Box for Inhibitors with Dual Efficacy against Giardia Lamblia and Cryptosporidium Parvum.” *PLoS Neglected Tropical Diseases* 12 (8): e0006673. https://doi.org/10.1371/journal.pntd.0006673.
Hopper, Allen T., Adam Brockman, Andy Wise, Julie Gould, Jennifer Barks, Joshua B. Radke, L. David Sibley, Yongmao Zou, and Stephen Thomas. 2019. “Discovery of Selective Toxoplasma Gondii Dihydrofolate Reductase Inhibitors for the Treatment of Toxoplasmosis.” *Journal of Medicinal Chemistry* 62 (3): 1562–76. https://doi.org/10.1021/acs.jmedchem.8b01754.
Hortua Triana, Miryam Andrea, Daniela Cajiao Herrera, Barbara H. Zimmermann, Barbara A. Fox, and David J. Bzik. 2016. “Pyrimidine Pathway-Dependent and -Independent Functions of the Toxoplasma Gondii Mitochondrial Dihydroorotate Dehydrogenase.” *Infection and Immunity* 84 (10): 2974–81. https://doi.org/10.1128/IAI.00187-16.
Hulverson, Matthew A., Igor Bruzual, Erin V. McConnell, Wenlin Huang, Rama S. R. Vidadala, Ryan Choi, Samuel L. M. Arnold, et al. 2019. “Pharmacokinetics and In Vivo Efficacy of Pyrazolopyrimidine, Pyrrolopyrimidine, and 5-Aminopyrazole-4-Carboxamide Bumped Kinase Inhibitors against Toxoplasmosis.” *The Journal of Infectious Diseases* 219 (9): 1464–73. https://doi.org/10.1093/infdis/jiy664.
Hyde, John E. 2007. “Targeting Purine and Pyrimidine Metabolism in Human Apicomplexan Parasites.” *Current Drug Targets* 8 (1): 31–47. https://doi.org/10.2174/138945007779315524.
Ineichen, Benjamin V., Serena Di Palma, Endre Laczko, Shane A. Liddelow, Susanne Neumann, Martin E. Schwab, and Alice C. Mosberger. 2020. “Regional Differences in Penetration of the Protein Stabilizer Trimethoprim (TMP) in the Rat Central Nervous System.” *Frontiers in Molecular Neuroscience* 13 (September): 167. https://doi.org/10.3389/fnmol.2020.00167.
John, Beena, Tajie H. Harris, Elia D. Tait, Emma H. Wilson, Beth Gregg, Lai Guan Ng, Paulus Mrass, et al. 2009. “Dynamic Imaging of CD8+ T Cells and Dendritic Cells during Infection with Toxoplasma Gondii.” *PLoS Pathogens* 5 (7): e1000505. https://doi.org/10.1371/journal.ppat.1000505.
Johnson, Steven M., Ryan C. Murphy, Jennifer A. Geiger, Amy E. DeRocher, Zhongsheng Zhang, Kayode K. Ojo, Eric T. Larson, et al. 2012. “Development of Toxoplasma Gondii Calcium-Dependent Protein Kinase 1 (TgCDPK1) Inhibitors with Potent Anti-Toxoplasma Activity.” *Journal of Medicinal Chemistry* 55 (5): 2416–26. https://doi.org/10.1021/jm201713h.
Katlama, C., S. De Wit, E. O’Doherty, M. Van Glabeke, and N. Clumeck. 1996. “Pyrimethamine-Clindamycin vs. Pyrimethamine-Sulfadiazine as Acute and Long-Term

Therapy for Toxoplasmic Encephalitis in Patients with AIDS." *Clinical Infectious Diseases: An Official Publication of the Infectious Diseases Society of America* 22 (2): 268–75. https://doi.org/10.1093/clinids/22.2.268.

Katlama, C., B. Mouthon, D. Gourdon, D. Lapierre, and F. Rousseau. 1996. "Atovaquone as Long-Term Suppressive Therapy for Toxoplasmic Encephalitis in Patients with AIDS and Multiple Drug Intolerance. Atovaquone Expanded Access Group." *AIDS* 10 (10): 1107–12. https://www.ncbi.nlm.nih.gov/pubmed/8874627.

Kim, Haeun, Brianne J. Burkinshaw, Linh G. Lam, Kevin Manera, and Tao G. Dong. 2021. "Identification of Small Molecule Inhibitors of the Pathogen Box against Vibrio Cholerae." *Microbiology Spectrum* 9 (3): e0073921. https://doi.org/10.1128/Spectrum.00739-21.

Konstantinovic, Neda, Hélène Guegan, Tijana Stäjner, Sorya Belaz, and Florence Robert-Gangneux. 2019. "Treatment of Toxoplasmosis: Current Options and Future Perspectives." *Food and Waterborne Parasitology* 15 (June): e00036. https://doi.org/10.1016/j.fawpar.2019.e00036.

Kovacs, J. A. 1992. "Efficacy of Atovaquone in Treatment of Toxoplasmosis in Patients with AIDS." *The Lancet* 340 (8820): 637–38. https://doi.org/10.1016/0140-6736(92)92172-C.

Lin, San San, Uwe Gross, and Wolfgang Bohne. 2009. "Type II NADH Dehydrogenase Inhibitor 1-Hydroxy-2-Dodecyl-4(1H)quinolone Leads to Collapse of Mitochondrial Inner-Membrane Potential and ATP Depletion in Toxoplasma Gondii." *Eukaryotic Cell* 8 (6): 877–87. https://doi.org/10.1128/EC.00381-08.

Lipinski, C. A., F. Lombardo, B. W. Dominy, and P. J. Feeney. 2001. "Experimental and Computational Approaches to Estimate Solubility and Permeability in Drug Discovery and Development Settings." *Advanced Drug Delivery Reviews* 46 (1-3): 3–26. https://doi.org/10.1016/s0169-409x(00)00129-0.

Maclean, Andrew E., Hannah R. Bridges, Mariana F. Silva, Shujing Ding, Jana Ovciarikova, Judy Hirst, and Lilach Sheiner. 2021. "Complexome Profile of Toxoplasma Gondii Mitochondria Identifies Divergent Subunits of Respiratory Chain Complexes Including New Subunits of Cytochrome bc1 Complex." *PLoS Pathogens* 17 (3): e1009301. https://doi.org/10.1371/journal.ppat.1009301.

MacRae, James I., Lilach Sheiner, Amsha Nahid, Christopher Tonkin, Boris Striepen, and Malcolm J. McConville. 2012. "Mitochondrial Metabolism of Glucose and Glutamine Is Required for Intracellular Growth of Toxoplasma Gondii." *Cell Host & Microbe* 12 (5): 682–92. https://doi.org/10.1016/j.chom.2012.09.013.

McConnell, Erin V., Igor Bruzual, Sovitj Pou, Rolf Winter, Rozalia A. Dodean, Martin J. Smilkstein, Alina Krollenbrock, et al. 2018. "Targeted Structure-Activity Analysis of Endochin-like Quinolones Reveals Potent Qi and Qo Site Inhibitors of Toxoplasma Gondii and Plasmodium Falciparum Cytochrome bc1 and Identifies ELQ-400 as a Remarkably Effective Compound against Acute Experimental Toxoplasmosis." *ACS Infectious Diseases* 4 (11): 1574–84. https://doi.org/10.1021/acsinfecdis.8b00133.

McFadden, D. C., S. Tomavo, E. A. Berry, and J. C. Boothroyd. 2000. "Characterization of Cytochrome B from Toxoplasma Gondii and Q(o) Domain Mutations as a Mechanism of Atovaquone-Resistance." *Molecular and Biochemical Parasitology* 108 (1): 1–12. https://doi.org/10.1016/s0166-6851(00)00184-5.

McHardy, N., L. S. Wekesa, A. T. Hudson, and A. W. Randall. 1985. "Antitheilerial Activity of BW720C (buparvaquone): A Comparison with Parvaquone." *Research in Veterinary Science* 39 (1): 29–33. https://www.ncbi.nlm.nih.gov/pubmed/3929346.

Meneceur, Pascale, Marie-Anne Bouldouyre, Dominique Aubert, Isabelle Villena, Jean Menotti, Virginie Sauvage, Jean-François Garin, and Francis Derouin. 2008. "In Vitro Susceptibility of Various Genotypic Strains of Toxoplasma Gondii to Pyrimethamine, Sulfadiazine, and Atovaquone." *Antimicrobial Agents and Chemotherapy* 52 (4): 1269–77. https://doi.org/10.1128/AAC.01203-07.

Metsalu, Tauno, and Jaak Vilo. 2015. "ClustVis: A Web Tool for Visualizing Clustering of Multivariate Data Using Principal Component Analysis and Heatmap." *Nucleic Acids Research* 43 (W1): W566–70. https://doi.org/10.1093/nar/gkv468.

Montazeri, Mahbobeh, Saeed Mehrzadi, Mehdi Sharif, Shahabeddin Sarvi, Shayesteh Shahdin, and Ahmad Daryani. 2018. "Activities of Anti-Toxoplasma Drugs and

Compounds against Tissue Cysts in the Last Three Decades (1987 to 2017), a Systematic Review." *Parasitology Research* 117 (10): 3045–57. https://doi.org/10.1007/s00436-018-6027-z.

Montazeri, Mahbobeh, Tahereh Mikaeili Galeh, Mahmood Moosazadeh, Shahabeddin Sarvi, Samira Dodangeh, Javad Javidnia, Mehdi Sharif, and Ahmad Daryani. 2020. "The Global Serological Prevalence of Toxoplasma Gondii in Felids during the Last Five Decades (1967-2017): A Systematic Review and Meta-Analysis." *Parasites & Vectors* 13 (1): 82. https://doi.org/10.1186/s13071-020-3954-1.

Montoya, J. G., and O. Liesenfeld. 2004. "Toxoplasmosis." *The Lancet* 363 (9425): 1965–76. https://doi.org/10.1016/S0140-6736(04)16412-X.

Müller, Joachim, Adriana Aguado-Martinez, Vera Manser, Vreni Balmer, Pablo Winzer, Dominic Ritler, Isabel Hostettler, David Arranz-Solís, Luis Ortega-Mora, and Andrew Hemphill. 2015. "Buparvaquone Is Active against Neospora Caninum in Vitro and in Experimentally Infected Mice." *International Journal for Parasitology, Drugs and Drug Resistance* 5 (1): 16–25. https://doi.org/10.1016/j.ijpddr.2015.02.001.

Nair, Sethu C., Carrie F. Brooks, Christopher D. Goodman, Angelika Sturm, Geoffrey I. McFadden, Sandeep Sundriyal, Justin L. Anglin, Yongcheng Song, Silvia N. J. Moreno, and Boris Striepen. 2012. "Apicoplast Isoprenoid Precursor Synthesis and the Molecular Basis of Fosmidomycin Resistance in Toxoplasma Gondii." *The Journal of Experimental Medicine* 209 (5): 1051–1051. https://doi.org/10.1084/jem.201100392095c.

Ngcongco, Khanyisile. 2020. "Evaluation of an NADPH-Dependent Assay for Inhibition Screening of Salmonella Enterica DOXP Reguctoisomerase for Identification of Novel Drug Hit Compounds." Rhodes University. https://commons.ru.ac.za/vital/access/services/Download/vital:41440/SOURCE1.

Nixon, G. L., D. M. Moss, A. E. Shone, D. G. Lalloo, and N. Fisher. 2013. "O, Neill, PM; Ward, SA; Biagini, GA." *The Journal of Antimicrobial Chemotherapy*.

Nugraha, Arifin Budiman, Bumduuren Tuvshintulga, Azirwan Guswanto, Dickson Stuart Tayebwa, Mohamed Abdo Rizk, Sambuu Gantuya, Gaber El-Saber Batiha, et al. 2019. "Screening the Medicines for Malaria Venture Pathogen Box against Piroplasm Parasites." *International Journal for Parasitology, Drugs and Drug Resistance* 10 (August): 84–90. https://doi.org/10.1016/j.ijpddr.2019.06.004.

Partridge, Frederick A., Anwen E. Brown, Steven D. Buckingham, Nicky J. Willis, Graham M. Wynne, Ruth Forman, Kathryn J. Else, et al. 2018. "An Automated High-Throughput System for Phenotypic Screening of Chemical Libraries on C. Elegans and Parasitic Nematodes." *International Journal for Parasitology, Drugs and Drug Resistance* 8 (1): 8–21. https://doi.org/10.1016/j.ijpddr.2017.11.004.

Rollin-Pinheiro, Rodrigo, Luana Pereira Borba-Santos, Mariana Ingrid Dutra da Silva Xisto, Yuri de Castro-Almeida, Victor Pereira Rochetti, Sonia Rozental, and Eliana Barreto-Bergter. 2021. "Identification of Promising Antifungal Drugs against Scedosporium and Lomentospora Species after Screening of Pathogen Box Library." *Journal of Fungi (Basel, Switzerland)* 7 (10). https://doi.org/10.3390/jof7100803.

Saleh, Ahmad, Johannes Friesen, Stefan Baumeister, Uwe Gross, and Wolfgang Bohne. 2007. "Growth Inhibition of Toxoplasma Gondii and Plasmodium Falciparum by Nanomolar Concentrations of 1-Hydroxy-2-Dodecyl-4(1H)quinolone, a High-Affinity Inhibitor of Alternative (type II) NADH Dehydrogenases." *Antimicrobial Agents and Chemotherapy* 51 (4): 1217–22. https://doi.org/10.1128/AAC.00895-06.

Schindelin, Johannes, Ignacio Arganda-Carreras, Erwin Frise, Verena Kaynig, Mark Longair, Tobias Pietzsch, Stephan Preibisch, et al. 2012. "Fiji: An Open-Source Platform for Biological-Image Analysis." *Nature Methods* 9 (7): 676–82. https://doi.org/10.1038/nmeth.2019.

Shaker, Bilal, Myeong-Sang Yu, Jin Sook Song, Sunjoo Ahn, Jae Yong Ryu, Kwang-Seok Oh, and Dokyun Na. 2020. "LightBBB: Computational Prediction Model of Blood–brain-Barrier Penetration Based on LightGBM." *Bioinformatics* 37 (8): 1135–39. https://doi.org/10.1093/bioinformatics/btaa918.

Sharifiyazdi, Hassan, Fatemah Namazi, Ahmad Oryan, Reza Shahriari, and Mostafa Razavi. 2012. "Point Mutations in the Theileria Annulata Cytochrome B Gene Is Associated with

Buparvaquone Treatment Failure." *Veterinary Parasitology* 187 (3-4): 431–35. https://doi.org/10.1016/j.vetpar.2012.01.016.
Shiomi, K., T. Kiyono, K. Okamura, M. Uezumi, Y. Goto, S. Yasumoto, S. Shimizu, and N. Hashimoto. 2011. "CDK4 and Cyclin D1 Allow Human Myogenic Cells to Recapture Growth Property without Compromising Differentiation Potential." *Gene Therapy* 18 (9): 857–66. https://doi.org/10.1038/gt.2011.44.
Shukla, Anurag, Kellen L. Olszewski, Manuel Llinás, Leah M. Rommereim, Barbara A. Fox, David J. Bzik, Dong Xia, et al. 2018. "Glycolysis Is Important for Optimal Asexual Growth and Formation of Mature Tissue Cysts by Toxoplasma Gondii." *International Journal for Parasitology* 48 (12): 955–68. https://doi.org/10.1016/j.ijpara.2018.05.013.
Smith, David, Geetha Kannan, Isabelle Coppens, Fengrong Wang, Hoa Mai Nguyen, Aude Cerutti, Einar B. Olafsson, et al. 2021. "Toxoplasma TgATG9 Is Critical for Autophagy and Long-Term Persistence in Tissue Cysts." *eLife* 10 (April). https://doi.org/10.7554/eLife.59384.
Songsungthong, Warangkhana, Sunisa Prasopporn, Louise Bohan, Potjanee Srimanote, Ubolsree Leartsakulpanich, and Suganya Yongkiettrakul. 2021. "A Novel Bicyclic 2,4-Diaminopyrimidine Inhibitor of Streptococcus Suis Dihydrofolate Reductase." *PeerJ* 9 (February): e10743. https://doi.org/10.7717/peerj.10743.
Songsungthong, Warangkhana, Suganya Yongkiettrakul, Louise E. Bohan, Eric S. Nicholson, Sunisa Prasopporn, Pimchai Chaiyen, and Ubolsree Leartsakulpanich. 2019. "Diaminoquinazoline MMV675968 from Pathogen Box Inhibits Acinetobacter Baumannii Growth through Targeting of Dihydrofolate Reductase." *Scientific Reports* 9 (1): 15625. https://doi.org/10.1038/s41598-019-52176-8.
Song, Zehua, Bogdan I. Iorga, Pierre Mounkoro, Nicholas Fisher, and Brigitte Meunier. 2018. "The Antimalarial Compound ELQ-400 Is an Unusual Inhibitor of the bc1 Complex, Targeting Both Qo and Qi Sites." *FEBS Letters* 592 (8): 1346–56. https://doi.org/10.1002/1873-3468.13035.
Spalenka, Jérémy, Sandie Escotte-Binet, Ali Bakiri, Jane Hubert, Jean-Hugues Renault, Frédéric Velard, Simon Duchateau, Dominique Aubert, Antoine Huguenin, and Isabelle Villena. 2018. "Discovery of New Inhibitors of Toxoplasma Gondii via the Pathogen Box." *Antimicrobial Agents and Chemotherapy* 62 (2). https://doi.org/10.1128/AAC.01640-17.
Sun, Lijun, Jiaxi Wu, Fenghe Du, Xiang Chen, and Zhijian J. Chen. 2013. "Cyclic GMP-AMP Synthase Is a Cytosolic DNA Sensor That Activates the Type I Interferon Pathway." *Science* 339 (6121): 786–91. https://doi.org/10.1126/science.1232458.
Thomsen-Zieger, Nadine, Joachim Schachtner, and Frank Seeber. 2003. "Apicomplexan Parasites Contain a Single Lipoic Acid Synthase Located in the Plastid." *FEBS Letters* 547 (1-3): 80–86. https://doi.org/10.1016/s0014-5793(03)00673-2.
Vallières, Cindy, Nicholas Fisher, Thomas Antoine, Mohammed Al-Helal, Paul Stocks, Neil G. Berry, Alexandre S. Lawrenson, et al. 2012. "HDQ, a Potent Inhibitor of Plasmodium Falciparum Proliferation, Binds to the Quinone Reduction Site of the Cytochrome bc1 Complex." *Antimicrobial Agents and Chemotherapy* 56 (7): 3739–47. https://doi.org/10.1128/AAC.00486-12.
Veale, Clinton G. L. 2019. "Unpacking the Pathogen Box-an Open Source Tool for Fighting Neglected Tropical Disease." *ChemMedChem* 14 (4): 386–453. https://doi.org/10.1002/cmdc.201800755.
Vercesi, A. E., C. O. Rodrigues, S. A. Uyemura, L. Zhong, and S. N. Moreno. 1998. "Respiration and Oxidative Phosphorylation in the Apicomplexan Parasite Toxoplasma Gondii." *The Journal of Biological Chemistry* 273 (47): 31040–47. https://doi.org/10.1074/jbc.273.47.31040.
Vila, Taissa, and Jose L. Lopez-Ribot. 2017. "Screening the Pathogen Box for Identification of Candida Albicans Biofilm Inhibitors." *Antimicrobial Agents and Chemotherapy* 61 (1). https://doi.org/10.1128/AAC.02006-16.
Wang, Jin-Lei, Si-Yang Huang, Michael S. Behnke, Kai Chen, Bang Shen, and Xing-Quan Zhu. 2016. "The Past, Present, and Future of Genetic Manipulation in Toxoplasma Gondii." *Trends in Parasitology* 32 (7): 542–53. https://doi.org/10.1016/j.pt.2016.04.013.
Wang, Peiyan, Siji Li, Yingchi Zhao, Baohuan Zhang, Yunfei Li, Shengde Liu, Hongqiang Du,

et al. 2019. “The GRA15 Protein from Toxoplasma Gondii Enhances Host Defense Responses by Activating the Interferon Stimulator STING.” *The Journal of Biological Chemistry* 294 (45): 16494–508. https://doi.org/10.1074/jbc.RA119.009172.

Weiss, Louis M., and Jitender P. Dubey. 2009. “Toxoplasmosis: A History of Clinical Observations.” *International Journal for Parasitology* 39 (8): 895–901. https://doi.org/10.1016/j.ijpara.2009.02.004.

Winzer, Pablo, Joachim Müller, Adriana Aguado-Martínez, Mahbubur Rahman, Vreni Balmer, Vera Manser, Luis Miguel Ortega-Mora, et al. 2015. “In Vitro and In Vivo Effects of the Bumped Kinase Inhibitor 1294 in the Related Cyst-Forming Apicomplexans Toxoplasma Gondii and Neospora Caninum.” *Antimicrobial Agents and Chemotherapy* 59 (10): 6361–74. https://doi.org/10.1128/AAC.01236-15.

Zampieri, Mattia, Michael Zimmermann, Manfred Claassen, and Uwe Sauer. 2017. “Nontargeted Metabolomics Reveals the Multilevel Response to Antibiotic Perturbations.” *Cell Reports* 19 (6): 1214–28. https://doi.org/10.1016/j.celrep.2017.04.002.